

Mimetic Inflation

Seyed Ali Hosseini Mansoori ^{a1}, Alireza Talebian ^{b2}, Hassan Firouzjahi ^{b3}

^a*Faculty of Physics, Shahrood University of Technology, P.O. Box 3619995161 Shahrood, Iran*

^b*School of Astronomy, Institute for Research in Fundamental Sciences (IPM), P.O. Box 19395-5531, Tehran, Iran*

ABSTRACT: We study inflationary solution in an extension of mimetic gravity with the higher derivative interactions coupled to gravity. Because of the higher derivative interactions the setup is free from the ghost and gradient instabilities while it hosts a number of novel properties. The dispersion relation of scalar perturbations develop quartic momentum correction similar to the setup of ghost inflation. Furthermore, the tilt of tensor perturbations can take either signs with a modified consistency relation between the tilt and the amplitude of tensor perturbations. Despite the presence of higher derivative interactions coupled to gravity the tensor perturbations propagate with the speed equal to the speed of light as required by the LIGO observations. Furthermore, the higher derivative interactions induce non-trivial interactions in cubic Hamiltonian, generating non-Gaussianities in various shapes such as the equilateral, orthogonal and squeezed configurations with observable amplitudes.

¹shosseini@shahroodut.ac.ir

²talebian@ipm.ir

³firouz@ipm.ir

Contents

1	Introduction	1
2	Inflationary Solution	3
3	Primordial Power Spectra	8
3.1	Scalar power spectrum	9
3.2	Tensor power spectrum	11
4	Primordial Bispectra	14
5	Summaries and Conclusions	18
A	Cosmological perturbations	20
A.1	Linear perturbations: Quadratic action	21
A.2	Nonlinear scalar perturbations: Cubic action	22
B	Explicit expressions for the amplitude of bispectrum	25
B.1	Expansion in terms of slow-roll parameters	27

1 Introduction

Mimetic gravity is a novel scalar-tensor theory proposed by Chamseddine and Mukhanov [1] as a modification of General Relativity (GR). The idea is to express the physical metric $g_{\mu\nu}$ in the Einstein-Hilbert action by performing a conformal transformation $g_{\mu\nu} = -(\tilde{g}^{\alpha\beta}\partial_\alpha\phi\partial_\beta\phi)\tilde{g}_{\mu\nu}$ from an auxiliary metric $\tilde{g}_{\mu\nu}$ in which ϕ is a scalar field. As a result, the longitudinal mode of gravity becomes dynamical even in the absence of any matter source. The above transformation can also be considered as a singular limit of the general disformal transformation where the transformation is not invertible [2, 3]. With the physical metric, the scalar field is subject to the constraint¹,

$$g^{\mu\nu}\partial_\mu\phi\partial_\nu\phi = -1. \tag{1.1}$$

As a consequence of this constraint, the theory mimics the roles of cold dark matter in cosmic expansion, hence the theory is dubbed as the mimetic dark matter. The original mimetic model was then extended to inflation, dark energy and also theories with non-singular cosmological and black hole solutions [4–6]. See also Refs. [7–37] for further theoretical developments in mimetic gravity.

¹We use the mostly positive signature for the metric.

The original version of the mimetic theory is free from instabilities [38, 39], but there is no nontrivial dynamics for scalar-type fluctuations. In order to circumvent this problem, the higher derivative term $(\square\phi)^2$ is added to the original action which generates a dynamical scalar degree of freedom propagating with a nonzero sound speed [4, 7]. In addition, the mimetic model with a general higher derivative function in the form $f(\square\phi)$ has been considered in Refs. [5, 6]. However, these extended mimetic setups with a propagating scalar degree of freedom are plagued with the ghost and the gradient instabilities [40–42]². To remedy these issues, it was suggested in [50–52] to extend the mimetic model further by considering direct couplings of the higher derivative terms to the curvature tensor of the spacetime such as $\square\phi R$, $\nabla_\mu\nabla_\nu\phi R^{\mu\nu}$, $\square\phi\nabla_\mu\phi\nabla_\nu\phi R^{\mu\nu}$ and so on. By appropriate choices of these higher derivative couplings one can bypass the problems of the gradient and the ghost instabilities. However, now the background dynamics is more complicated and a simple dark matter solution is not a direct outcome of the analysis.

In this work our goal is to construct inflationary solutions in the extended mimetic setup with the effects of higher derivative couplings taking into account. As we will see the presence of higher derivative couplings to gravity generate new interactions and the analysis of cosmological perturbations become non-trivial. For example, because of these higher derivative interactions the dispersion relation of scalar perturbations receive higher order corrections resembling non-relativistic dispersion relation as in ghost inflation setup [53]. In addition, the predictions for the tensor perturbations are modified with a new consistency condition between the scalar spectral index n_s , the sound speed of scalar perturbations c_s and the tensor to scalar ratio r_t .

Because of the higher derivative interactions, the model predicts novel non-Gaussianity features. The situation here is somewhat similar to the EFT studies of higher derivative corrections to the single field model [54] where large non-Gaussianity of various shapes such as equilateral and orthogonal types can be generated. In addition, similar to models with a non-standard kinetic energy such as DBI model [55], the sound speed of scalar perturbations play non-trivial roles in generating large non-Gaussianities. The strong observational bounds on primordial non-Gaussianities can be used to constrain the model parameters. More specifically, the amplitude of non-Gaussianity parameter f_{NL} in the squeezed, equilateral and orthogonal configurations from the Planck observations [56, 57] are constrained to be

$$f_{\text{NL}}^{\text{sq}} = -0.9 \pm 5.1, \quad f_{\text{NL}}^{\text{equi}} = -26 \pm 47, \quad f_{\text{NL}}^{\text{ortho}} = -38 \pm 24 \quad (68\% \text{CL}). \quad (1.2)$$

We shall use these bounds to constrain model parameters and various couplings.

The organization of the paper is as follows. In next Section, we present our setup and construct the background solutions which mimic cold dark matter even in the absence of normal matter. Then we extend these analysis to obtain an inflationary solution. In Section 3 we obtain the power spectrum of the curvature and tensor perturbations and calculate

²The mimetic dark matter scenario also suffers from caustics [43], see also [44–47]. It should be noted that the gauge field extensions of the mimetic scenario potentially avoid caustics formations [48, 49].

various cosmological observables. In Section 4, we study bispectrum and calculate the non-Gaussianity parameter f_{NL} for local, equilateral and orthogonal configurations numerically, followed by discussions and summaries in Section 5. Many technical analysis of cosmological perturbations associated to power spectra and scalar bispectrum are relegated to Appendices A and B.

2 Inflationary Solution

In this section we study the background dynamics to obtain a period of inflation in early universe.

As summarized in Introduction, to remedy the ghost and gradient instabilities various higher derivative terms are added to the mimetic setup. Besides the higher derivative terms such as $(\square\phi)^2$ and $\nabla_\mu\nabla_\nu\phi\nabla^\mu\nabla^\nu\phi$, we also require the higher derivative couplings of the mimetic field to the curvature of the spacetime such as $\square\phi R$, $\nabla_\mu\nabla_\nu\phi R^{\mu\nu}$, $\square\phi\nabla_\mu\phi\nabla_\nu\phi R^{\mu\nu}$ and so on [50–52]. Here we restrict ourselves to the simplest case where there is only a direct coupling of the higher derivative term $\square\phi \equiv \chi$ to the Ricci scalar as follows,

$$S = \int d^4x \sqrt{-g} \left[\frac{M_{\text{P}}^2}{2} F(\chi) R + \lambda \left(g^{\alpha\beta} \partial_\alpha \phi \partial_\beta \phi + 1 \right) + P(\chi) - V(\phi) \right], \quad (2.1)$$

in which M_{P} is the reduced Planck mass³. The Lagrangian multiplier λ enforces the constraint Eq. (1.1) [59]. In addition, we have allowed a potential term for the mimetic field which will drive inflation. In this setup P and F are arbitrary smooth function of χ . The former is added to make the scalar perturbation propagating (i.e. inducing a non-zero c_s) while the latter is required to remedy the gradient and the ghost instabilities [50–52]. As mentioned before, more complicated function of derivatives of ϕ and χ such as $F_2(\nabla_\mu\nabla_\nu\phi R^{\mu\nu})$ and $F_3(\chi\nabla_\mu\phi\nabla_\nu\phi R^{\mu\nu})$ can also be added along with the simple function $F(\chi)$. However, the analysis even in the simplest setup of action (2.1) is complicated enough so we do not consider models with other higher derivative couplings.

Before presenting the fields equation one important comment is in order. In the action (2.1) the effective gravitational coupling (effective reduced Planck mass) is actually $M_{\text{P}} F(\chi)^{1/2}$. We can perform the calculations in the given ‘‘Jordan frame’’ but with a proper interpretation of the physical gravitational coupling. Alternatively, we may perform a metric field redefinition and go to the ‘‘Einstein frame’’ where the gravitational coupling is simply M_{P} . The latter is rather complicated as the model presented in action (2.1) contains various higher derivative terms. Instead, we follow the first approach and work in the original Jordan frame. However, we make a further assumption that at the end of inflation the fields ϕ becomes trivial with $F(\chi_e) = 1$ and one recovers the standard GR afterwards. This is a simplification made based on the intuitive ground though we do not have a dynamical mechanism to enforce it. We leave it as an open question as how or whether this transition from a mimetic setup to a

³The Hamiltonian analysis of this model have also been investigated in Ref [58] in both Einstein frame and Jordan frame.

standard GR setup can be achieved at the end of inflation. With these discussions in mind, we set $M_P = 1$ in the rest of the analysis.

By taking the variation of the action (2.1) with respect to the inverse metric $g^{\mu\nu}$, one obtains the Einstein field equations as $F(\chi)G_{\mu\nu} = T_{\mu\nu}$ where $G_{\mu\nu}$ is the Einstein tensor and $T_{\mu\nu}$ is the effective energy momentum tensor, given by

$$T_\nu^\mu = -2\lambda\partial^\mu\phi\partial_\nu\phi + \left[\partial^\mu P_\chi\partial_\nu\phi + \partial^\mu\phi\partial_\nu P_\chi + \frac{1}{2}\left(\partial^\mu\phi\partial_\nu(RF_\chi) + \partial_\nu\phi\partial^\mu(RF_\chi)\right) + \nabla^\mu\partial_\nu F \right] + \delta_\nu^\mu \left[P - \chi P_\chi - V - g^{\alpha\beta}\partial_\alpha P_\chi\partial_\beta\phi - \frac{1}{2}\nabla^\alpha\left(R\partial_\alpha\phi F_\chi\right) + \square F \right], \quad (2.2)$$

in which $P_\chi \equiv \partial P/\partial\chi$ and so on. In obtaining the above expression we have implemented the mimetic constraint (1.1). Clearly the energy momentum tensor given above can not be cast into the form of the energy momentum tensor of a perfect fluid.

Moreover, varying the action (2.1) with respect to the scalar field ϕ gives the following modified Klein-Gordon equation,

$$\frac{1}{\sqrt{-g}}\partial_\mu\left[\sqrt{-g}\left(2\lambda\partial^\mu\phi - \partial^\mu\left(P_\chi + \frac{1}{2}RF_\chi\right)\right)\right] + \frac{\partial V(\phi)}{\partial\phi} = 0. \quad (2.3)$$

The background cosmological solution is in the form of FRLW universe with the metric

$$ds^2 = -dt^2 + a(t)^2 d\mathbf{x}^2, \quad (2.4)$$

in which t and a are the cosmic time and the scale factor respectively. One can check that the background field equations take the following forms

$$3FH^2 = V - 2\lambda - (P + 3HP_\chi + 3\dot{H}P_{\chi\chi}) - 3\left(6H^3F_\chi - 4H\dot{H}F_\chi + 6H^2\dot{H}F_{\chi\chi} + 3\dot{H}^2F_{\chi\chi} - \ddot{H}F_\chi\right), \quad (2.5)$$

and

$$F(2\dot{H} + 3H^2) = V - (P + 3HP_\chi - 3\dot{H}P_{\chi\chi}) - 3H\left(F_\chi(6H^2 + 5\dot{H}) - 6H\dot{H}F_{\chi\chi}\right), \quad (2.6)$$

where $H = \dot{a}(t)/a(t)$ is the Hubble expansion rate. Note that at the background level, the mimetic constraint (1.1) enforces $\dot{\phi} = 1$ and correspondingly $\chi = -3H$.

Before constructing the inflationary solution, let us for the moment set $V = 0$ to see how the mimetic setup can yield the dark matter solution. Using Eq. (2.3) the Lagrangian multiplier is obtained as follows

$$\lambda = \frac{\mathcal{C}}{2a^3} + 6H\dot{H}F_\chi - 9H^2\dot{H}F_{\chi\chi} - \frac{9}{2}\dot{H}^2F_{\chi\chi} - \frac{3}{2}\dot{H}P_{\chi\chi} + \frac{3}{2}\ddot{H}F_\chi \quad (V = 0), \quad (2.7)$$

in which \mathcal{C} is an integration constant. Plugging this into the Friedmann equation (2.5), one obtains

$$\frac{3H^2}{2}\left[F + 6HF_\chi + \frac{1}{3H^2}(P + 3HP_\chi)\right] = -\frac{\mathcal{C}}{a^3} \quad (V = 0). \quad (2.8)$$

The constant \mathcal{C} above indicates that a dark matter type solution can exist. However, in order for this conclusion to be valid we require the combination in the big bracket in Eq. (2.8) to be a constant. Since this combination plays important roles in our analysis below let us define

$$F + 6HF_\chi + \frac{1}{3H^2}(P + 3HP_\chi) \equiv -\mathcal{K}. \quad (2.9)$$

Using this definition of the function \mathcal{K} and taking the time derivative of Eq. (2.8) once more, we obtain

$$2\dot{H} + 3H^2 = -\frac{H\dot{\mathcal{K}}}{\mathcal{K}}, \quad (V = 0). \quad (2.10)$$

For a dark matter solution with $a \sim t^{2/3}$, the left hand side of Eq. (2.10) vanishes so indeed to have a dark matter solution we require the function \mathcal{K} to be constant. In this case the Friedmann equation simplifies to $3H^2 = \tilde{\mathcal{C}}/a^3 = \rho$ where ρ is the effective energy density and $\tilde{\mathcal{C}} \equiv 2\mathcal{C}/\mathcal{K}$. To have a consistent solution one requires that $\tilde{\mathcal{C}} > 0$ while there is no restriction on the signs of \mathcal{C} and \mathcal{K} separately at this level. For example, in the original mimetic setup with $F = 1$ and $P = 0$, one obtains $\mathcal{K} = -1$ and the dark matter solution is a direct outcome of the analysis. In conclusion, while the functions $P(\chi)$ and $F(\chi)$ are arbitrary, but in order to obtain a dark matter candidate in this setup one requires the combination \mathcal{K} defined in Eq. (2.9) to be a constant.

Now we consider the case when $V(\phi) = V(t) \neq 0$ in order to obtain inflationary solution. Starting with the second Einstein equation (2.6) and using the definition of \mathcal{K} to eliminate the combinations containing $F_{\chi\chi}$ and $P_{\chi\chi}$ in favours of $\dot{\mathcal{K}}$ we obtain

$$2\dot{H} + 3H^2 = -\frac{H\dot{\mathcal{K}}}{\mathcal{K}} + \frac{V}{\mathcal{K}}. \quad (2.11)$$

In particular, if we set $V = 0$, we recover Eq. (2.10) as expected. Now noting that

$$2\dot{H} + 3H^2 + \frac{H\dot{\mathcal{K}}}{\mathcal{K}} = \frac{1}{a^3 H^2 \mathcal{K}} \frac{d}{dt} \left(a^3 H^2 \mathcal{K} \right), \quad (2.12)$$

we can integrate Eq. (2.11) to obtain

$$3H^2 = \frac{1}{\mathcal{K} a^3} \left(\mathcal{C} - 3 \int da a^2 V \right), \quad (2.13)$$

in which as in previous case \mathcal{C} is a constant.

In an inflationary background one can neglect the constant term \mathcal{C} in Eq. (2.13) as it is diluted rapidly. In addition, if V is nearly flat as in conventional slow-roll scenarios then we can obtain a phase of near dS spacetime with $H^2 \simeq -V/\mathcal{K}$. Now we see the curious effect that in order to obtain an inflationary background we require the signs of V and \mathcal{K} to be opposite. However, as we shall see in next section, in order to have healthy scalar and tensor perturbations we require $\mathcal{K} > 0$. As a result, to obtain an inflationary solution in this setup we need a negative potential. This should be compared with the analysis in [4] where $F = 1$,

$P(\chi) = \frac{\gamma}{2}\chi^2$ and $V > 0$. For these values of F and P we obtain $\mathcal{K} = -1 + 3\gamma/2$. On the other hand, the sound speed of scalar perturbations in the model of [4] is $c_s^2 = \gamma/(2 - 3\gamma)$ so \mathcal{K} has opposite sign compared to c_s^2 (with $\gamma > 0$). Now in order to avoid the gradient instability one requires $c_s^2 > 0$ so in their inflationary solution they need $\mathcal{K} < 0$. But as we shall see in next section the sign of the quadratic action for the scalar perturbations is proportional to the sign of \mathcal{K} so a negative \mathcal{K} indicates the propagation of ghost as pointed out in details in [41]. As we mentioned above, this problem arises because in the analysis of [4] they considered $V > 0$ to construct inflationary solution.

Although the mimetic field ϕ is not an ordinary ‘‘rolling’’ scalar field in the sense that it appears with a constraint in the setup, but the requirement of a negative potential looks unexpected. However, we remind that negative potentials have been employed in the past in other contexts such as in contracting universes [60–64], see also [65, 66].

To construct a specific inflationary setup, we consider the inverted quadratic potential as follows

$$V(\phi) = \begin{cases} -\frac{1}{2}m^2\phi^2 & t < 0 \\ 0 & t > 0 \end{cases}, \quad \phi = t \quad (2.14)$$

Inflation occurs when $t < 0$ while the hot big bang phase follows inflation for $t > 0$. We obtain the inflationary phase as the field rolls up the negative potential toward the origin. In addition, we assume that the potential vanishes for $t > 0$, so as discussed below Eq. (2.10), the seeds of observed dark matter can be obtained in this setup when inflation ends.

So far our analysis were general and we did not specify the forms of the functions $F(\chi)$ and $P(\chi)$, unless we require the combination \mathcal{K} to be positive. From now on, we further demand that \mathcal{K} is a constant which simplifies the construction of the inflationary solution greatly. Now by introducing the new variable $y \equiv a^{\frac{3}{2}}$, Eq. (2.11) becomes a linear differential equation,

$$\ddot{y} - \frac{3m^2t^2}{8\mathcal{K}}y = 0, \quad (t < 0) \quad (2.15)$$

which is similar to Eq. (31) in Ref. [4].

The inflationary branch of the solution is given by

$$y(t) = \sqrt{-t} K_{\frac{1}{4}}\left(\sqrt{\frac{3}{32\mathcal{K}}} m t^2\right), \quad (2.16)$$

in which $K_\nu(x)$ is the modified Bessel function of the second kind. At large negative t , one finds that the scale factor grows as

$$a \propto (-t)^{-\frac{1}{3}} \exp\left(-\frac{mt^2}{2\sqrt{6\mathcal{K}}}\right), \quad (2.17)$$

whereas it is proportional to $(t)^{2/3}$ for positive t after inflation which is the indication of a dark matter dominated universe. Of course, we have to include reheating where radiation should be generated after inflation.

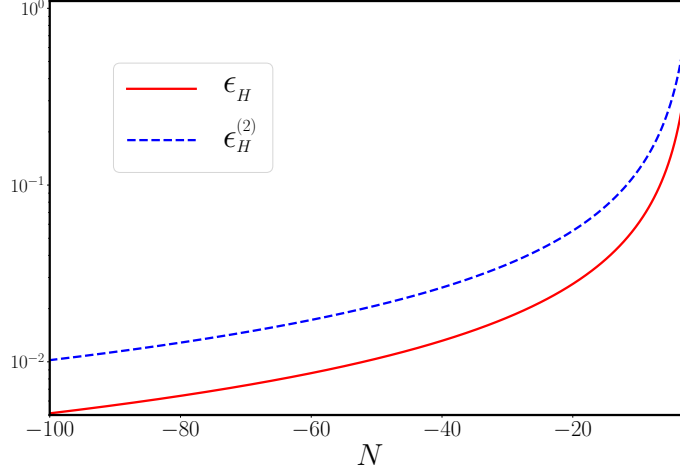


Figure 1. The first and second slow-roll parameters associated to the scale factor (2.17) in terms of the number of e-folds N . These behaviours are independent from the values of m and \mathcal{K} .

The behaviours of the corresponding slow-roll parameters,

$$\epsilon_H \equiv -\frac{\dot{H}}{H^2}, \quad \epsilon_H^{(2)} \equiv \frac{\dot{\epsilon}_H}{H \epsilon_H}, \quad (2.18)$$

are shown in Fig. 1. One can easily satisfy the conditions $\epsilon_H, \epsilon_H^{(2)} \ll 1$ to obtain 50 – 60 number of e-folds to solve the flatness and the horizon problems. As usual, inflation ends when either of the slow-roll parameters approach order of unity. It should be noted that these slow-roll conditions are independent of the values of m and \mathcal{K} .

For the future uses, let us define the slow-roll parameters associated with the background functions such as H, F etc as follows

$$\epsilon_X^{(1)} \equiv \epsilon_X \equiv \pm \frac{\dot{X}}{H X} \quad \text{and} \quad \epsilon_X^{(n)} \equiv \frac{\dot{\epsilon}_X^{(n-1)}}{H \epsilon_X^{(n-1)}} \quad \text{for } n \geq 2. \quad (2.19)$$

Note that the minus sign is chosen when $X = H$ while for other background functions we chose the plus sign. Using the scale factor (2.17) in the inflationary phase, we find the following relations among the Hubble slow-roll parameters:

$$\epsilon_H^{(4)} \approx \epsilon_H^{(3)} \approx \epsilon_H^{(2)} \approx 2\epsilon_H \approx \left| \frac{1}{N} \right| \ll 1, \quad (2.20)$$

which are satisfied for $N \sim 50 - 60$ number of e-folds before the end of inflation.

As mentioned before, our functions $F(\chi)$ and $P(\chi)$ are arbitrary except that we have imposed that the combination \mathcal{K} defined in Eq. (2.9) to be constant. For example, the following pair of the polynomial functions

$$F(\chi) = 1 + \alpha\chi + \beta\chi^2, \quad P(\chi) = \frac{\gamma}{2}\chi^2 - \frac{\alpha}{6}\chi^3 - \frac{\beta}{3}\chi^4,$$

satisfy the constraint (2.9) with $\mathcal{K} = -1 + 3\gamma/2$.

In general case, the polynomial functions $F(\chi) = \sum_{n=0} f_n \chi^n$, and $P(\chi) = \sum_{n=0} p_n \chi^n$ can be considered with $p_0 = 0$ and p_1 an arbitrary constant. If the rest of coefficients f_n and p_n satisfy the relations $p_2 \neq \frac{f_0}{3}$ and

$$p_{n+2} = \frac{1-2n}{3n+3} f_n \quad n \geq 1, \quad (2.21)$$

then we obtain $\mathcal{K} = 3p_2 - f_0$.

One open question in this setup is the issue of reheating after inflation. To be consistent with the big bang cosmology, the inflationary phase has to be followed by a hot radiation dominated background. In conventional slow-roll models this is achieved via the (p)reheating mechanism in which the inflaton field transfers its energy to the Standard Model (SM) particles and fields while oscillating in its global minimum. In our mimetic scenario the field ϕ is not a rolling field in the usual sense but instead it is a space-filling field with the profile $\phi = t$. So in order to achieve reheating one has to modify the current setup and couple the mimetic field to the SM fields one way or another. This is an open question which deserves a separate study elsewhere. We also comment that in the current setup with the potential (2.14) a dark matter solution is inherited in the solution for $t > 0$ so one may only need reheating to generate the host radiation while the dark matter can come from the mimetic source.

3 Primordial Power Spectra

In this section we calculate the power spectra of the curvature and tensor perturbations. For this purpose we calculate the quadratic actions associated to these perturbations.

The details of the analysis of the quadratic actions are presented in Appendix A. The quadratic action for the comoving curvature perturbation \mathcal{R} and the tensor perturbations γ_{ij} is obtained to be

$$S_2 = \int dt d^3\mathbf{x} \vartheta \frac{a^3}{2} \left[\dot{\mathcal{R}}^2 - \frac{c_s^2}{a^2} (\partial\mathcal{R})^2 - \sigma^2 \left(\frac{\partial^2 \mathcal{R}}{a^2} \right)^2 + \frac{F}{4\vartheta} \left((\dot{\gamma}_{ij})^2 - \frac{(\partial\gamma_{ij})^2}{a^2} \right) \right]. \quad (3.1)$$

in which we have defined the parameters ϑ and σ as

$$\vartheta \equiv \frac{3\mathcal{K}F}{\mathcal{K}+F}, \quad \sigma^2 \equiv \frac{F_\chi^2}{\mathcal{K}F}, \quad (3.2)$$

and during inflation the sound speed of scalar perturbations c_s^2 as

$$c_s^2 \equiv -\frac{1}{3\mathcal{K}} (\mathcal{K} + F + 3HF_\chi). \quad (3.3)$$

Note that ϑ is dimensionless while σ has the dimension of length square.

In order for the perturbations to be free from the ghost and gradient instabilities we require that all three parameters ϑ , c_s^2 and σ^2 to be positive. Correspondingly we require

$$\mathcal{K} > 0, \quad F > 0, \quad F_\chi < 0. \quad (3.4)$$

In particular note that if $\mathcal{K} < 0$ then the scalar perturbations develop ghost instability. This is the reason why we needed to couple the higher derivative terms to gravity to cure the ghost and gradient instabilities in the original setup of mimetic gravity [50–52].

3.1 Scalar power spectrum

The quadratic action for the scalar perturbations from the quadratic action (3.1) in Fourier space can be written as

$$S_{\text{Scalar}}^{(2)} = \frac{1}{2} \int d\tau d^3k \left[(u'_k)^2 - \left(c_s^2 k^2 + \frac{\sigma^2}{a^2} k^4 - \frac{\ddot{z}''}{\dot{z}} \right) u_k^2 \right]. \quad (3.5)$$

in which the prime indicates the derivative with respect to the conformal time $d\tau = dt/a(t)$ and we have defined the canonically normalized field $u \equiv z\mathcal{R}$ with $z \equiv \sqrt{\vartheta}a$.

In a near de Sitter background where ϑ , c_s and σ are approximately constant⁴ we have $z''/z \simeq 2/\tau^2$ and the corresponding mode function equation is given by

$$u_k'' + \left(\omega(\tau)^2 - \frac{2}{\tau^2} \right) u_k = 0; \quad \omega(\tau)^2 \equiv c_s^2 k^2 + \sigma^2 H^2 k^4 \tau^2. \quad (3.6)$$

The above equation indicates that we are dealing with a modified dispersion relation. With $\mathcal{K} > 0$ we have $\sigma^2 > 0$ and the dispersion relation (3.6) is known as the Corley-Jacobson dispersion relation which was studied for investigating the black holes physics [68, 69] and for the effects of trans-Planckian physics on cosmological perturbations [70, 71]. In addition, this type of dispersion relation occurs in ghost inflation [53] where a timelike scalar field fills the entire spacetime with the profile $\phi = t$ as in our mimetic setup.

Such modified dispersion relations indicate the violation of Lorentz invariance in the UV limit. However, for low physical momentum when

$$\frac{k}{a} \ll \frac{c_s}{\sigma}, \quad (3.7)$$

the linear dispersion relation is recovered. We can define the scale at which the modification to the linear dispersion relation becomes important as $\Lambda \equiv c_s/\sigma$. For the physical momentum larger than this scale, $k_{\text{phy}} \gtrsim \Lambda$, the quartic contribution to the dispersion relation becomes important. For future purpose we introduce the parameter ν via

$$\nu \equiv \frac{c_s^{-1} H}{\Lambda} = \frac{\sigma H}{c_s^2}, \quad (3.8)$$

which quantifies the ratio of the sound-Hubble horizon parameter over the momentum scale Λ around when the behaviour of the dispersion relation changes. For the models in which $\nu \ll 1$ the dispersion relation is a linear relation, $\omega \propto k$, as in standard slow-roll models, while for $\nu \gg 1$ the mode function u_k is described by the non-relativistic dispersion relation $\omega \propto k^2$.

⁴The mode equation (3.6) was extensively analyzed without any approximations in Ref. [67].

Imposing the adiabatic vacuum initial conditions, the mode function of the comoving curvature perturbation is obtained to be [72–74]

$$\mathcal{R}(\mathbf{k}, \tau) = w_k(\tau)a_{\mathbf{k}} + w_k^*(\tau)a_{-\mathbf{k}}^\dagger; \quad w_k(\tau) = \frac{iH\sqrt{\tau}e^{-\frac{\pi}{8\nu}}}{c_s k \sqrt{2\nu\vartheta}} W_{\frac{i}{4\nu}, \frac{3}{4}}(-i\nu c_s^2 k^2 \tau^2), \quad (3.9)$$

where $a_{\mathbf{k}}$ and $a_{\mathbf{k}}^\dagger$ are the creation and the annihilation operators as usual and $W_{\frac{i}{4\nu}, \frac{3}{4}}$ is the Whittaker function.

With the help of the above mode function, it is easy to calculate the super horizon ($c_s k \tau \rightarrow 0$) limit of the power-spectrum for comoving curvature perturbation. Taking into account the asymptotic behaviour of Whittaker function, i.e. $W_{a,b}(z) \approx z^{1/2-b}\Gamma(2b)/\Gamma(b-a+1/2)$ for $z \rightarrow 0$ [75], the curvature perturbations power spectrum on superhorizon scales is given by

$$\mathcal{P}_{\mathcal{R}} = \frac{1}{16\pi c_s^3} \frac{H^2}{\vartheta} g(\nu); \quad g(\nu) \equiv \frac{\nu^{-3/2} e^{-\frac{\pi}{4\nu}}}{|\Gamma(\frac{5}{4} + \frac{i}{4\nu})|^2}. \quad (3.10)$$

Let us now discuss about the asymptotic behaviour of the the power spectrum in small and large ν limits. In the limit $\nu \ll 1$ ⁵, we find out

$$\mathcal{P}_{\mathcal{R}} \simeq \frac{1}{4\pi^2 c_s^3} \frac{H^2}{\vartheta} \left(1 - \frac{5}{4}\nu^2\right). \quad (3.11)$$

Since in the limit $\nu \ll 1$ we have a relativistic dispersion relation, one expects that the power spectrum in this limit resembles that of standard slow-roll inflation. Indeed, if we formally identify the coefficient ϑ in the quadratic action (3.1) with the corresponding factor in the action of slow-roll models [76], $\vartheta \leftrightarrow 2\epsilon_H/c_s^2$, then the power spectrum in Eq. (3.11) reduces to the standard result $\mathcal{P}_{\mathcal{R}} = H^2/8\pi^2\epsilon_H c_s$ in slow-roll models.

On the other hand, in the limit $\nu \gg 1$ the quartic term k^4 dominates in ω^2 and the dispersion relation becomes non-relativistic as in the model of ghost inflation [53]. In this limit the power spectrum (3.10) reduces to

$$\mathcal{P}_{\mathcal{R}} = \frac{H^{1/2}\sigma^{-3/2}}{\pi\vartheta\Gamma(\frac{1}{4})^2}. \quad (3.12)$$

Identifying a suitable choice of the parameters ϑ and σ with the corresponding parameters in [53] we reproduce the power spectrum for ghost inflation as well.

Having calculated the curvature perturbation power spectrum, we can also calculate the spectral index n_s as

$$n_s - 1 = \left. \frac{d \ln \mathcal{P}_{\mathcal{R}}}{d \ln k} \right|_* \simeq -2\epsilon_H - 3\epsilon_{c_s} - \epsilon_\vartheta + \epsilon_g, \quad (3.13)$$

where the subscript $*$ shows the time of horizon crossing for the mode of interest k and we have used our slow-roll notation (2.19) for the background variables $X = c_s, \vartheta, g(\nu)$. In order to have an almost scale invariant power spectrum, one requires the four parameters ϵ_H , ϵ_ϑ , ϵ_{c_s} , and ϵ_g to be very small.

⁵We use the relation $|\Gamma(x+iy)| \sim \sqrt{2\pi} |y|^{x-1/2} e^{-\pi|y|/2}$ as $y \rightarrow \infty$.

3.2 Tensor power spectrum

To calculate the power spectrum of tensor perturbations, let us first expand the tensor modes of the quadratic action (3.1) in terms of their polarization tensors e_{ij}^+ and e_{ij}^\times as $\gamma_{ij} = \sum_{+, \times} \gamma^\lambda e_{ij}^\lambda$ where $\lambda = +, \times$ and e_{ij}^λ are symmetric, transverse and traceless tensors. Moreover, using the normalization condition, $e_{ij}^\lambda e_{ij}^{\lambda'} = 2\delta_{\lambda\lambda'}$, we obtain the second-order action for the tensor modes in Fourier space as follows

$$S_{\text{Tensor}}^{(2)} = \frac{1}{2} \sum_{\lambda} \int d\tau d^3k \tilde{z}^2 \left(\gamma_\lambda'^2 - k^2 \gamma_\lambda^2 \right), \quad (3.14)$$

where $\tilde{z}^2 \equiv F(\chi) a^2/2$. In order for the perturbation to be stable, we require that $F > 0$.

Interestingly, from the above action we see that the tensor modes propagate with the speed equal to unity, $c_T = 1$, i.e. the tensor perturbations propagate with the speed of light. This is because we considered the special case of higher derivative coupling to gravity in the form of $F(\chi)$. However, it is well-known that for general higher derivative interactions with gravity, c_T is not equal to speed of light. These types of modified gravity theories are under strong constraints from the LIGO observations which require that $|c_T - 1| < 5 \times 10^{-15}$ [77–79]. For example, in our setup if we allow more general higher derivative interactions such as the curvature independent quadratic higher derivative terms $\nabla_\mu \nabla_\nu \phi \nabla^\mu \nabla^\nu \phi$ and the curvature dependent cubic higher derivative terms $\square \phi \nabla^\mu \phi \nabla^\nu \phi R_{\mu\nu}$ and $\nabla^\mu \nabla^\nu \phi R_{\mu\nu}$ then $c_T \neq 1$ [48].

Upon defining the canonically normalized field associated with γ_λ by $v_\lambda \equiv \tilde{z} \gamma_\lambda$ and imposing the the Minkowski (Bunch-Davies) initial condition, the mode function is obtained to be

$$\gamma_\lambda(\tau, \mathbf{k}) = \frac{iH e^{-ik\tau}}{k^{3/2} \sqrt{2F}} (1 + ik\tau). \quad (3.15)$$

Defining the power spectrum of the gravitational tensor modes via

$$\sum_{\lambda} \langle \gamma^\lambda \gamma^\lambda \rangle \equiv \frac{2\pi^2}{k^3} \mathcal{P}_\gamma (2\pi)^3 \delta^{(3)}(\mathbf{k} - \mathbf{k}'), \quad (3.16)$$

we obtain

$$\mathcal{P}_\gamma = \frac{2H^2}{\pi^2 F}, \quad (3.17)$$

where both H and F are evaluated at the time of horizon crossing. Compared to conventional models of inflation, we see the additional factor $1/F$ in tensor power spectrum. This is understandable if one notes that, naively speaking, we have rescaled the gravitational coupling $M_{\text{P}}^2 \rightarrow M_{\text{P}}^2 F$ in the starting action Eq. (2.1).

The spectral index of \mathcal{P}_γ is also given by

$$n_t \equiv \left. \frac{d \ln \mathcal{P}_\gamma}{d \ln k} \right|_* = -2\epsilon_H - \epsilon_F \quad (3.18)$$

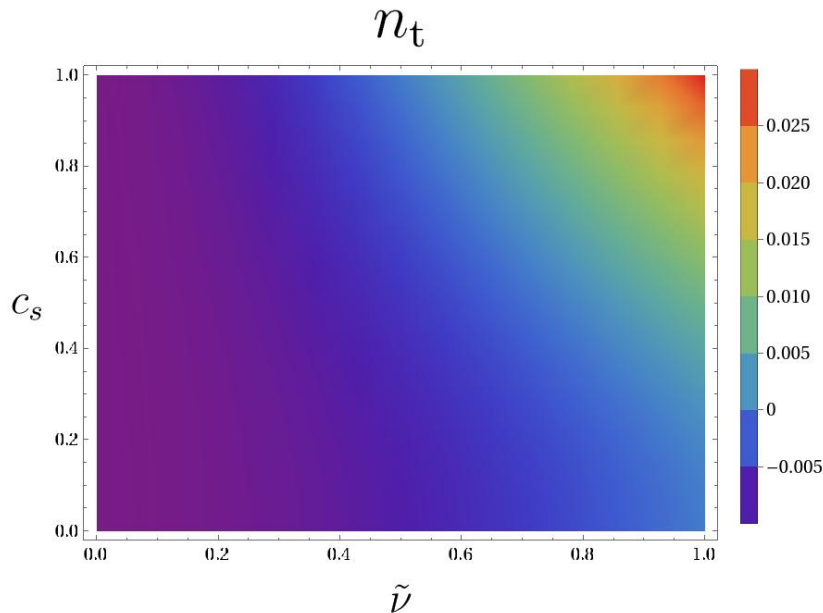


Figure 2. The density plot of n_t versus c_s and $\tilde{\nu} \equiv \sqrt{\mathcal{K}/F}$. We have taken $\epsilon_H = 0.01$.

where ϵ_F is the slow-roll parameter associated with F as defined in Eq. (2.19) which is given by

$$\epsilon_F \equiv \frac{\dot{F}}{H F} = -\frac{3HF\chi}{F} \epsilon_H = -\epsilon_H \left[1 + \tilde{\nu}^2 (1 + 3c_s^2) \right], \quad (3.19)$$

where $\tilde{\nu} \equiv \sqrt{\mathcal{K}/F}$ and we have used Eq. (3.3) in the last step. In particular, we see that n_t depends on c_s and $\tilde{\nu}$ after plugging the slow parameter ϵ_F from Eq. (3.19) into Eq. (3.18).

In Fig. 2 we have presented the predictions for n_t for some values of $(c_s, \tilde{\nu})$ in the parameter space. Interestingly, we see that in some regions of parameter space $n_t > 0$, i.e. the tensor power spectrum is blue-tilted. This is unlike the conventional slow-roll models which generally predict a red-tilted tensor power spectrum. As is the case in our model, the detection of a blue-tilted tensor perturbations cannot rule out inflation automatically [60, 80, 81].

As long as we assume $\tilde{\nu} \lesssim \mathcal{O}(\sqrt{\epsilon_H})$, then Eq. (3.19) guarantees that $\epsilon_F \simeq -\epsilon_H$ in the subluminal regime with $0 < c_s < 1$. It means that the function $F(\chi)$ changes very slowly during slow-roll inflation. Therefore, we can consider it approximately as a constant during inflation. To estimate this value, let us first define the tensor to scalar ratio as follows,

$$r_t \equiv \frac{\mathcal{P}_\gamma}{\mathcal{P}_\mathcal{R}} = \frac{32c_s^3 \vartheta}{\pi F g(\nu)}. \quad (3.20)$$

Then, by restoring M_{P} in the scalar and tensor power spectra and using the current observational constraint on inflationary parameters [56], i.e. $r_t \lesssim 0.056$ and $\mathcal{P}_\mathcal{R} \simeq 2.1 \times 10^{-9}$, the

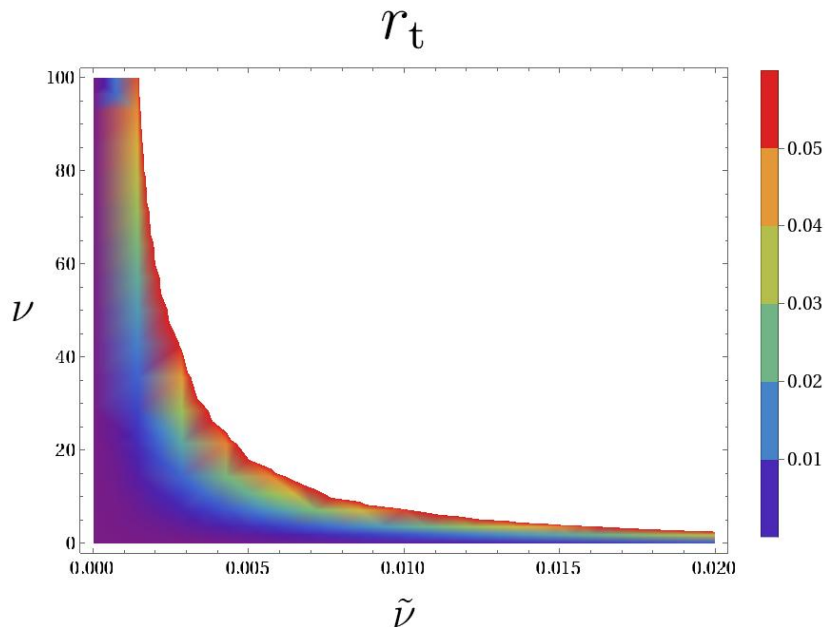


Figure 3. The density plot of r_t versus ν and $\tilde{\nu}$ for $c_s = 1$. The white regions are excluded by the observational bound $r_t \leq 0.056$ [56].

value of F at horizon crossing can be estimated as

$$F_* = 1.72 \times 10^{-3} \left(\frac{r_t}{0.056} \right)^{-1} \left(\frac{H}{10^{-6} \text{ M}_\text{P}} \right)^2, \quad (3.21)$$

which implies that we need to choose $\mathcal{K} \lesssim 10^{-5}$ to satisfy the condition $\tilde{\nu} \lesssim \mathcal{O}(\sqrt{\epsilon_H})$. As mentioned before, the slow roll approximation $\epsilon_F \approx -\epsilon_H$ is valid only in the region where the comoving curvature perturbation propagates with $c_s < 1$. The superluminal propagation speed with $c_s > 1$ is not a problem per se as it does not directly violate causality on the background [82, 83]. However, we restrict ourselves to scalar perturbations with subluminal speeds.

Using Eqs. (3.19) and (3.18), we can also obtain the following generalized consistency relation between r_t and n_t ,

$$r_t = \frac{32c_s}{\pi g(v)(\tilde{\nu}^2 + 1)} \left(\frac{n_t}{\epsilon_H} + 1 - \tilde{\nu}^2 \right). \quad (3.22)$$

We see that the consistency relation in conventional models of inflation [84], $r_t = -8c_s n_t$, is modified in our model due to the mimetic constraint. In Fig. 3 we have presented the predictions for $r_t(\nu, \tilde{\nu})$ for $c_s = 1$. The white areas correspond to the regions of parameter space which are not allowed due to the observational bound $r_t \leq 0.056$ [56]. By choosing smaller values of c_s the allowed regions become more extended.

Before closing this section, here we compare our results for the inflationary background with those of [50]. We have shown that in order for a consistent inflationary solution to exist in this setup, the potential has to be negative. Then imposing the additional condition that the parameter \mathcal{K} defined in Eq. (2.9) be a constant we have verified the existence of a period of slow-roll inflation as demonstrated in Fig. 1. Then calculating the quadratic actions and performing the perturbation analysis we have shown that the spectral tilt of tensor perturbations can take either signs. On the other hand, Ref. [50] claimed the existence of slow-roll solution with a potential which is (implicitly) positive⁶. As for the predictions of the scalar and tensor power spectra they have borrowed the analysis of [67] which was in a different context. As a result, they have obtained the standard result $n_t = -2\epsilon_H$, so the tilt of tensor perturbations is always negative.

4 Primordial Bispectra

In this section, we calculate the three-point correlation of the scalar perturbations $\langle \mathcal{R}\mathcal{R}\mathcal{R} \rangle$ and look at the amplitudes and shapes of non-Gaussianity in various limits.

Utilizing the standard methods, the expectation value of the three point correlation is given by [85]

$$\langle \mathcal{R}(\mathbf{k}_1) \mathcal{R}(\mathbf{k}_2) \mathcal{R}(\mathbf{k}_3) \rangle = -i \int_{\tau_i}^{\tau_e} a \, d\tau \langle 0 | \left[\mathcal{R}(\tau_e, \mathbf{k}_1) \mathcal{R}(\tau_e, \mathbf{k}_2) \mathcal{R}(\tau_e, \mathbf{k}_3), H_{\text{int}} \right] | 0 \rangle, \quad (4.1)$$

where H_{int} is the interaction Hamiltonian which is calculated from expanding the Lagrangian (2.1) up to 3rd orders in curvature perturbations, given in (A.16), with $H_{\text{int}} = -\mathcal{L}_3$. Moreover, \mathbf{k}_i are the wave vectors and τ_i is the initial time when the inflationary perturbations are deep inside the Hubble radius. Since during a quasi-de Sitter expansion $\tau \simeq -1/(aH)$, it is a good approximation to calculate the integral in the limit $\tau_i \rightarrow -\infty$ and $\tau_e \rightarrow 0$.

In the Fourier space, we can write the three-point correlation function of curvature perturbations as

$$\langle \mathcal{R}(\mathbf{k}_1) \mathcal{R}(\mathbf{k}_2) \mathcal{R}(\mathbf{k}_3) \rangle \equiv (2\pi)^3 \delta^3(\mathbf{k}_1 + \mathbf{k}_2 + \mathbf{k}_3) \mathcal{B}_{\mathcal{R}}(k_1, k_2, k_3), \quad (4.2)$$

in which $k_i = |\mathbf{k}_i|$ and $B_{\mathcal{R}}(k_1, k_2, k_3)$ is called the bispectrum⁷ which can be parameterized as

$$B_{\mathcal{R}}(k_1, k_2, k_3) \equiv \frac{(2\pi)^4 \mathcal{P}_{\mathcal{R}}^2}{\prod_{n=1}^3 k_n^3} \mathcal{A}(k_1, k_2, k_3) \quad (4.3)$$

where \mathcal{A} is called the amplitude of bispectrum.

⁶There is a discrepancy with the signature of the action used in [50]. While they use the $(+, -, -, -)$ signature as in Chamseddine-Mukhanov [1], but their action has an opposite sign for the Einstein-Hilbert term. Fortunately, this sign discrepancy does not affect their perturbation analysis about the ghost/gradient instabilities but it has important effects when writing the background equation. More specifically, their potential should be replaced by $-V$.

⁷Because of the translational invariance, the total momentum $\mathbf{K} \equiv \mathbf{k}_1 + \mathbf{k}_2 + \mathbf{k}_3$ is conserved.

Finally, the non-linearity parameter f_{NL} associated with the amplitude of bispectrum is defined by the following relation

$$f_{\text{NL}} \equiv \frac{10}{3} \frac{1}{\sum_{i=1}^3 k_i^3} \mathcal{A}(k_1, k_2, k_3). \quad (4.4)$$

As we see from Eq. (A.16), our interaction Hamiltonian contains 22 independent terms (interactions). These complicated interactions originate from the higher derivative terms in $F(\chi)$ and $P(\chi)$. Each of them induce different shapes and amplitudes of non-Gaussianities.

As examples, let us calculate the bispectrum for the following two terms of the cubic action (A.16),

$$\mathcal{L}_{\text{int}} \supset f_2 \dot{\mathcal{R}} \frac{(\partial \mathcal{R})^2}{a^2} + f_8 \dot{\mathcal{R}}^3, \quad (4.5)$$

which also exist in the model of ghost inflation with the modified dispersion relation $\omega^2 \propto k^4$.

The bispectrum for each term in Eq. (4.5) is evaluated using the mode function of \mathcal{R} given in Eq. (3.9) as follows

$$\begin{aligned} \mathcal{B}_{\mathcal{R}}(k_1, k_2, k_3)_2 &= i f_2 w_{k_1}^*(0) w_{k_2}^*(0) w_{k_3}^*(0) \int_{-\infty}^0 d\tau \frac{1}{H\tau} w_{k_1}(\tau) w_{k_2}(\tau) w'_{k_3}(\tau) (\mathbf{k}_1 \cdot \mathbf{k}_2) \\ &+ \text{symm.} + \text{c.c.} \end{aligned} \quad (4.6)$$

and

$$\mathcal{B}_{\mathcal{R}}(k_1, k_2, k_3)_8 = 6i f_8 w_{k_1}^*(0) w_{k_2}^*(0) w_{k_3}^*(0) \int_{-\infty}^0 d\tau \frac{1}{H\tau} w'_{k_1}(\tau) w'_{k_2}(\tau) w'_{k_3}(\tau) + \text{c.c.} \quad (4.7)$$

Using the explicit expression for the wave function (3.9) and substituting the above results into Eq. (4.3) for \mathcal{A} , we obtain the following expressions for the amplitudes $\mathcal{A}^{(2)}$ and $\mathcal{A}^{(8)}$ associated with each interaction:

$$\mathcal{A}^{(2)} = \frac{f_2 H^5}{c_s^8 \mathcal{P}_{\mathcal{R}}^2 \vartheta^3} \sum_{i,j,l=1}^3 |\epsilon_{ijl}| \mathcal{I}_{1,-1}^{p_i, p_j, p_l}(\nu) k_i(\mathbf{k}_j \cdot \mathbf{k}_l), \quad (4.8)$$

with $p_1 = 1$ and $p_2 = p_3 = 0$, and

$$\mathcal{A}^{(8)} = \frac{6f_8 H^5}{c_s^6 \mathcal{P}_{\mathcal{R}}^2 \vartheta^3} k_1 k_2 k_3 \mathcal{I}_{0,-1}^{1,1,1}(\nu). \quad (4.9)$$

Here the function $\mathcal{I}_{n_1, n_2}^{p_1, p_2, p_3}$ is defined via

$$\mathcal{I}_{n_1, n_2}^{p_1, p_2, p_3}(\nu, k_1, k_2, k_3) \equiv \text{Re} \left[\alpha(\nu) \nu^{-(n_1 + \frac{3}{4})} \int_{-\infty}^0 dx x^{n_2} h_\nu^{(p_1)}(x) h_\nu^{(p_2)}\left(\frac{k_2}{k_1} x\right) h_\nu^{(p_3)}\left(\frac{k_3}{k_1} x\right) \right], \quad (4.10)$$

where

$$\alpha(\nu) \equiv \frac{15e^{\frac{(i-3)\pi}{8\nu}}}{7680\pi^{5/2}} \Gamma\left(\frac{5}{4} + \frac{i}{4\nu}\right)^{-3} \quad \text{and} \quad h_\nu(x) \equiv \frac{e^{-\frac{\pi}{8\nu}} \sqrt{x} W_{\frac{i}{4\nu}, \frac{3}{4}}(-ix^2)}{\nu^{3/4}}, \quad (4.11)$$

and the upper index p_i denotes the order of derivative with respect to the function variables. For example $h_\nu^{(0)}(x) = h_\nu(x)$, $h_\nu^{(1)}(x) = \frac{dh_\nu(x)}{dx}$ and so on. The amplitudes for all other interactions are listed in Appendix B.

To study the shape function of the above amplitudes, in Figs. 4 and 5 we have presented the 3D plot of $r_2^{-1}r_3^{-1}\mathcal{A}(1, r_2, r_3)$ as a function of $r_2 \equiv k_2/k_1$ and $r_3 \equiv k_3/k_2$ for $\nu = \{1, 10, 50\}$. The plots are produced numerically, after rotating the contour of integration over τ along the direction $\propto -(1+i)$ so that they converge exponentially. We see that $\mathcal{A}^{(2)}$ and $\mathcal{A}^{(8)}$ roughly have similar shapes and amplitudes and both roughly peak at the equilateral limit $k_1 = k_2 = k_3 = k$. In addition, the variation of ν has no significant effects on the shapes.

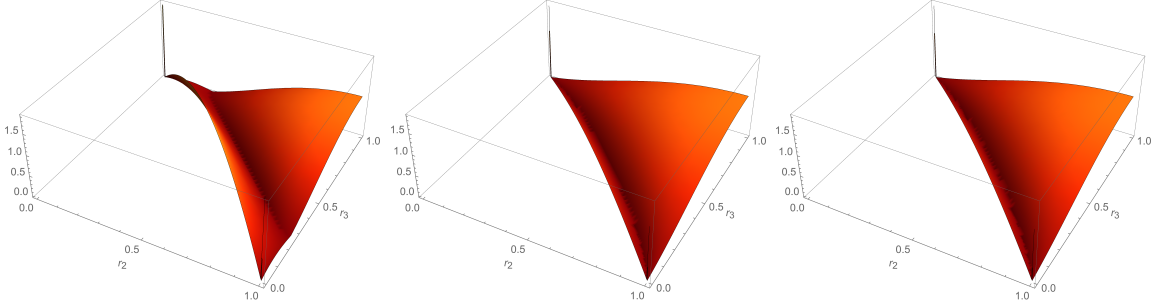


Figure 4. Numerical results for the shapes of $|\mathcal{A}^{(2)}|/k_1k_2k_3$ for $\nu = 1, 10, 50$ from left to right. The amplitude is normalized by the value obtained in the equilateral limit.

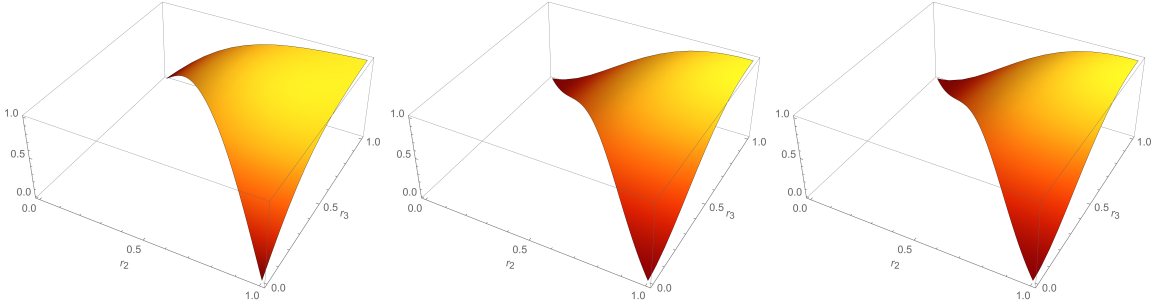


Figure 5. Numerical results for the shapes of $|\mathcal{A}^{(8)}|/k_1k_2k_3$ for $\nu = 1, 10, 50$ from left to right with the description as in Fig. 4.

In Table 1 we list the shape of each contribution presented in Appendix B. One can see that most of the non-Gaussianity shapes peak at the equilateral limit where all three modes have comparable wavelengths. However, some shapes are close to the orthogonal shape and the local shape which has a peak in the squeezed limit. For example, as shown in Fig. 6, $\mathcal{A}^{(4)}$ and $\mathcal{A}^{(10)}$ peak in the squeezed triangle limit ($k_3 \ll k_1 \simeq k_2$) and in orthogonal triangle limit ($k_3 = k_2 = k_1/2$), respectively.

Combining the contributions from all interactions listed in Appendix B, the total non-

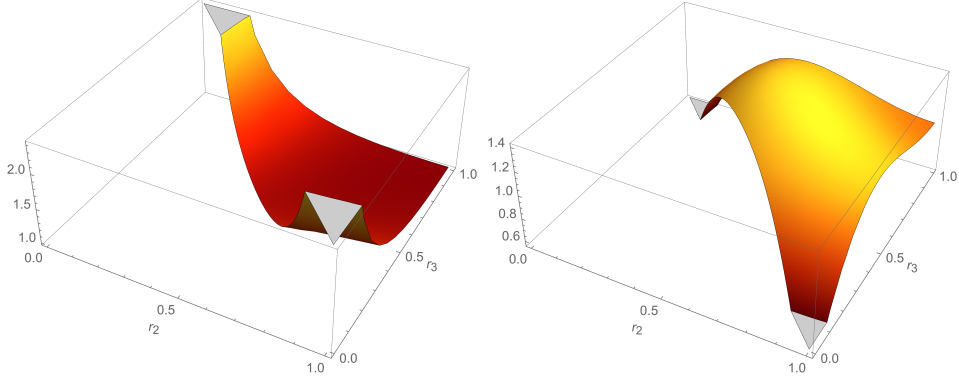


Figure 6. Numerical results for the shapes of $|\mathcal{A}^{(4)}|/k_1k_2k_3$ (left panel) and $|\mathcal{A}^{(10)}|/k_1k_2k_3$ (right panel) for $\nu = 1$. The amplitude is normalized by the value obtained in the equilateral limit.

Amplitude	$\mathcal{A}^{(1)}$	$\mathcal{A}^{(3)}$	$\mathcal{A}^{(4)}$	$\mathcal{A}^{(5)}$	$\mathcal{A}^{(6)}$	$\mathcal{A}^{(7)}$	$\mathcal{A}^{(9)}$	$\mathcal{A}^{(10)}$	$\mathcal{A}^{(11)}$	$\mathcal{A}^{(12)}$
Shape	Local	Equi	Local	Equi	Equi	Local	Equi	Ortho	Equi	Equi
Amplitude	$\mathcal{A}^{(13)}$	$\mathcal{A}^{(14)}$	$\mathcal{A}^{(15)}$	$\mathcal{A}^{(16)}$	$\mathcal{A}^{(17)}$	$\mathcal{A}^{(18)}$	$\mathcal{A}^{(19)}$	$\mathcal{A}^{(20)}$	$\mathcal{A}^{(21)}$	$\mathcal{A}^{(22)}$
Shape	Equi	Local	Equi	Equi	Equi	Equi	Equi	Equi	Ortho	Equi

Table 1. The shape of bispectrum for each interaction listed in Appendix. **B**.

Gaussianity parameter f_{NL} is given by

$$f_{\text{NL}} = \frac{10}{3} \frac{1}{\sum_{i=1}^3 k_i^3} \sum_{j=1}^{22} \mathcal{A}^{(j)}. \quad (4.12)$$

Correspondingly, we can calculate f_{NL} numerically for squeezed ($k_1 = k_2 = k, k_3 \rightarrow 0$), equilateral ($k_1 = k_2 = k_3 = k$) and orthogonal ($k_1 = k, k_2 = k_3 = k/2$) shapes.

In Figs. 7, 8, and 9, f_{NL} is presented in the various range of ν in the squeezed, equilateral and orthogonal configurations. It is worth mentioning that f_{NL} is controlled by three parameters, the sound speed c_s , the scalar to tensor ratio r_t and ν . In the left hand panels of these figures, f_{NL} can take the observationally allowed values in some range of ν by varying c_s while $r_t = 0.01$ is held fixed. A similar conclusion holds in the right hand panels where we fix $c_s = 1$ and vary r_t . Generally, f_{NL} increases by reducing c_s and r_t . One can find corners of parameter space which yield to acceptable amplitudes for f_{NL} as required by observations in Eq. (1.2).

For further studies of bispectrum and its expansion in terms of slow-roll parameters see Appendix B.1.

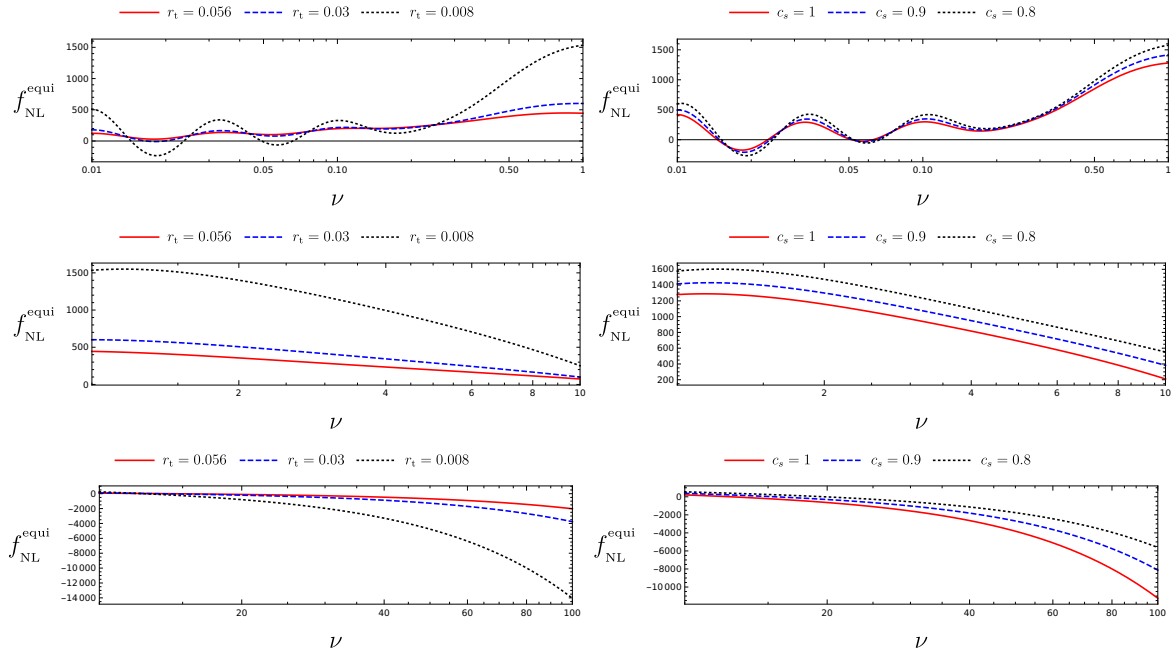


Figure 7. Numerical results for $f_{\text{NL}}^{\text{equi}}$ in the equilateral configuration with ν in the range $[0.01, 100]$. In the left panels we have fixed $c_s = 1$ while r_t is varied whereas in the right panels we have set $r_t = 0.01$ and c_s is varied.

5 Summaries and Conclusions

In this paper we have studied inflationary solution in an extension of mimetic gravity with higher derivative interactions coupled to gravity. It is known that the original mimetic setup is plagued with the ghost and gradient instabilities. These instabilities can be removed with the help of higher derivative interactions coupled to gravity. There are a number of options to include higher derivative corrections. In this paper we have studied the simplest higher derivative correction in the form $F(\chi)R$ with $\chi \equiv \square\phi$. It would be interesting to extend the current analysis to include other higher derivative terms coupled to gravity such as $F_2(\nabla_\mu\nabla_\nu\phi R^{\mu\nu})$, $F_3(\chi\nabla_\mu\phi\nabla_\nu\phi R^{\mu\nu})$ etc. In addition, in order for the scalar perturbations to become dynamical with a non-zero sound speed c_s we have included the term $P(\chi)$ as well.

One curious effect in our analysis is that in order to obtain an inflationary solution we have to work with a negative potential. This conclusion is a consequence of the fact that we deal with a constrained theory. More specifically, in order for the quadratic actions of the scalar and tensor perturbation to be free from instabilities the higher derivative functions $F(\chi)$ and $P(\chi)$ are subject to certain conditions which cause the potential to be negative. Inflation is achieved while the field rolls up the potential towards $V = 0$. While a negative potential may be considered problematic a priori but our analysis shows that the setup shows no pathologies either at the background or at the perturbation level.

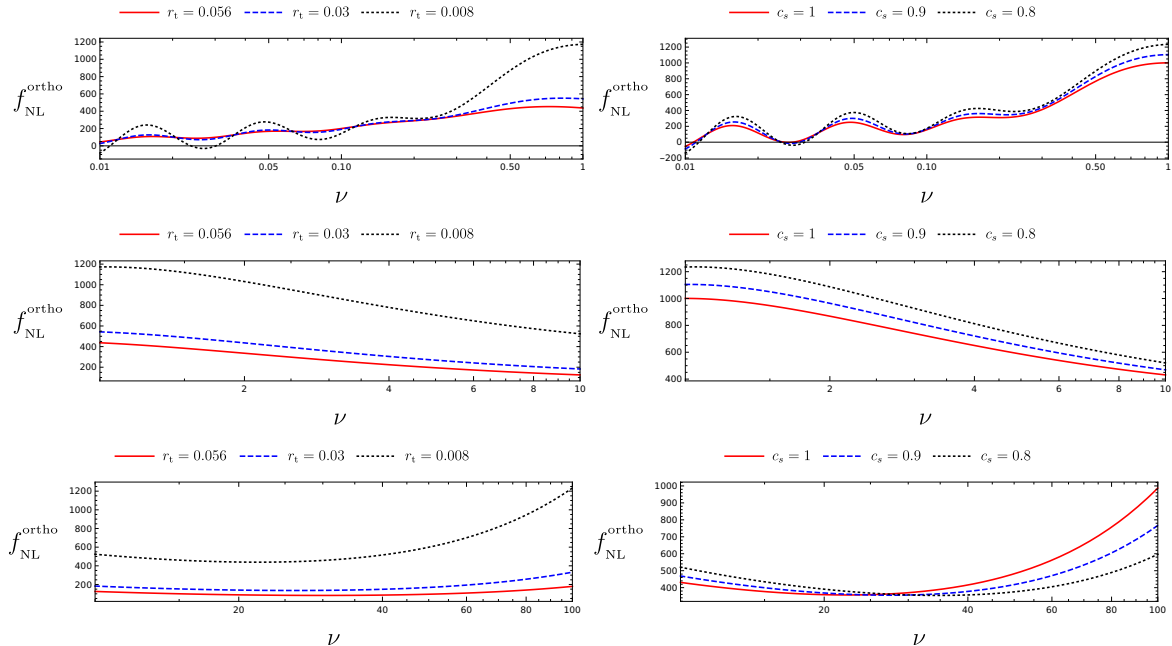


Figure 8. Numerical results for $f_{\text{NL}}^{\text{ortho}}$ in the range of $\nu = [0.01, 100]$ for orthogonal configuration. In the left panels we have considered $c_s = 1$, whereas in the right panels we have set $r_t = 0.01$.

While the background yields a period of slow-roll inflation the cosmological perturbations in this setup have novel behaviours. Because of the higher derivative interactions the dispersion relation associated with the scalar perturbations receives higher order momentum corrections as in the model of ghost inflation. Furthermore, the tilt of tensor perturbations can take either signs in contrast to conventional inflation models [85, 86]. In addition, we obtain a new consistency relation between r_t and n_t which involves c_s and other model parameters encoding the higher derivative interactions. Despite the presence of higher derivative corrections the tensor perturbations propagate with the speed equal to speed of light as strongly implied by the LIGO observations.

We also studied the predictions of this setup for the amplitudes and shapes of non-Gaussianities. Because of higher derivative interactions, various types of interactions are developed in the cubic action endowing the setup with rich non-Gaussianity properties. Depending on model parameters, large amplitudes of non-Gaussianities in various shapes such as equilateral, orthogonal and squeezed configurations are produced.

As we mentioned before, it is assumed that the effective Newton constant is stabilized after inflation, corresponding to $F(\chi_e) = 1$. We did not provide a dynamical mechanism for this important requirement. In addition, we have not specified the reheating mechanism in this setup. Indeed, it is possible that these two questions are related to each other. While this work was primarily concerned with cosmological perturbations such as the power spectrum and bispectrum, but a concrete picture requires that the questions of reheating and the stabilization

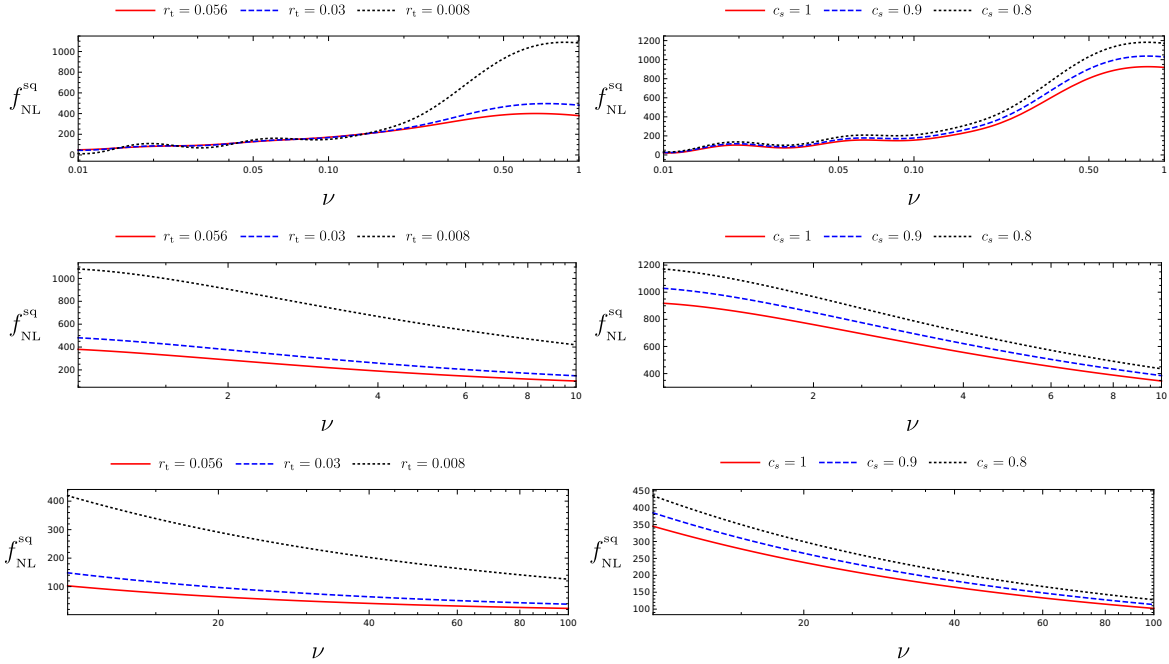


Figure 9. Numerical results for $f_{\text{NL}}^{\text{sq}}$ in the range of $\nu = [0.01, 100]$ for squeezed configuration. In the left panels we have considered $c_s = 1$, whereas in the right panels we have set $r_t = 0.01$.

of the effective Newton constant to be addressed as well. These are important questions which are beyond the scope of the current analysis.

Acknowledgements

We would like to thank Alireza Vafaei Sadr, Amin Farhang and Mehdi Atashi for helpful discussions on the numerical methods and Mohammad Ali Gorji for insightful discussions.

A Cosmological perturbations

In this Appendix we present the analysis of cosmological perturbations in comoving gauge in which the calculations are significantly simpler than other gauges. Moreover, this gauge is especially suitable for investigating the ghost and gradient instabilities. The special property of this gauge is that all perturbation are encoded in the metric sector while the scalar field is kept unperturbed, $\delta\phi(t, \vec{x}) = 0$.

Implementing the ADM formalism, the metric is decomposed as

$$ds^2 = -N^2 dt^2 + h_{ij}(dx^i + N^i dt)(dx^j + N^j dt) , \quad (\text{A.1})$$

in which N and N^i are the lapse function and the shift vector respectively while the three-dimensional metric h_{ij} determines the geometry of the spatial hypersurfaces. At the level of

background $N = 1$, $N_i = 0$ and $h_{ij} = a(t)^2 \delta_{ij}$. It is then possible to write down perturbations as follows,

$$N \equiv 1 + \alpha, \quad N_i \equiv \partial_i \psi, \quad h_{ij} \equiv a(t)^2 e^{2\mathcal{R}} \delta_{ij} + \gamma_{ij}, \quad (\text{A.2})$$

where α , ψ and \mathcal{R} are scalar perturbations. In addition, there is the scalar perturbation $\lambda = \lambda(t) + \delta\lambda(t, \vec{x})$ for the Lagrange multiplier.

Because of the global $O(3)$ symmetry, the scalar, vector and tensor perturbations decouple at the linear order of perturbations. Here we have ignored vector perturbations in Eq. (A.2) in view of the fact that the vector perturbations decay as usual in an expanding universe.

At this stage, the above perturbations must be substituted in the action (2.1) to extract the quadratic and cubic actions for the scalar and tensor perturbations. Before doing so, let us first impose the mimetic constraint Eq. (1.1) at the level of perturbations defined in Eq. (A.2) which yields

$$\alpha = 0. \quad (\text{A.3})$$

This result simplifies our following calculations considerably.

A.1 Linear perturbations: Quadratic action

Plugging the above perturbations into the action (2.1) and after some integration by parts, the quadratic action in comoving gauge for \mathcal{R} and γ_{ij} is obtained as follows

$$\begin{aligned} S_{\text{com}}^{(2)} = \int dt d^3 \mathbf{x} \frac{a^3}{2} \left\{ -3 \left(F + \frac{15}{2} H F_\chi - 9 H^2 F_{\chi\chi} \right) \left(\dot{\mathcal{R}}^2 + \mathcal{R} \dot{\mathcal{R}} \right) - 3 \mathcal{K} \mathcal{R} \dot{\mathcal{R}} - 2 F_\chi \partial^2 \psi \partial^2 \mathcal{R} \right. \\ \left. + \frac{(\partial \mathcal{R})^2}{a^2} \left(F + 3 H F_\chi - 9 \dot{H} F_{\chi\chi} \right) - 2 \mathcal{K} \partial^2 \psi \dot{\mathcal{R}} + \frac{1}{3} (\partial^2 \psi)^2 (\mathcal{K} + F) \right. \\ \left. + \frac{F}{4} \left[(\dot{\gamma}_{ij})^2 - \frac{(\partial \gamma_{ij})^2}{a^2} \right] \right\} \quad (\text{A.4}) \end{aligned}$$

where we have used Eq. (2.9) to simplify the result in terms of the function \mathcal{K} . Note that in the these analysis there is no assumption on the function \mathcal{K} so it is kept general.

It is evident that the ψ mode is a non dynamical degrees of freedom which can be integrated out from the action. Varying Eq. (A.4) with respect to ψ , we find

$$\partial^2 \psi = \frac{3}{\mathcal{K} + F} \left(\mathcal{K} \dot{\mathcal{R}} + F_\chi \frac{\partial^2 \mathcal{R}}{a^2} \right). \quad (\text{A.5})$$

Substituting the above result into the action (A.4) and after some integration by parts the quadratic Lagrangian in comoving gauge for \mathcal{R} and γ_{ij} is obtained to be

$$\mathcal{L}_2 = \vartheta \frac{a^3}{2} \left\{ \dot{\mathcal{R}}^2 - \frac{c_s^2}{a^2} (\partial \mathcal{R})^2 - \sigma^2 \left(\frac{\partial^2 \mathcal{R}}{a^2} \right)^2 + \frac{F}{4\vartheta} \left[(\dot{\gamma}_{ij})^2 - \frac{(\partial \gamma_{ij})^2}{a^2} \right] \right\}, \quad (\text{A.6})$$

in which we have defined

$$\vartheta \equiv \frac{3\mathcal{K}F}{\mathcal{K}+F}, \quad \sigma^2 \equiv \frac{F_\chi^2}{\mathcal{K}F}, \quad (\text{A.7})$$

and during inflation, the sound speed of the scalar perturbations c_s^2 as

$$c_s^2 \equiv -\frac{1}{3\mathcal{K}} (\mathcal{K} + F + 3HF_\chi). \quad (\text{A.8})$$

As discussed in the main text, in order to avoid the ghost and gradient instabilities we demand that $\vartheta > 0$, $c_s^2 > 0$ and $\sigma^2 > 0$. Applying these conditions on Eqs. (A.7) and (A.8), we obtain the following constraints

$$\mathcal{K} > 0, \quad F > 0, \quad F_\chi < 0. \quad (\text{A.9})$$

A.2 Nonlinear scalar perturbations: Cubic action

In this section, we calculate the cubic action for the scalar perturbations which is used to calculate the bispectrum.

Expanding the action (2.1) up to third order, the cubic action is given by

$$\begin{aligned} S_{\text{com}}^{(3)} = & \int dt d^3x a^3 \left\{ 9\mathcal{K} \mathcal{R} \dot{\mathcal{R}}^2 + \tilde{f}_1 \mathcal{R} \frac{(\partial\mathcal{R})^2}{a^2} - 9F_{\chi\chi} \dot{\mathcal{R}}^2 \frac{\partial^2\mathcal{R}}{a^2} - 6\mathcal{K} \left(\dot{\mathcal{R}} \partial_i \mathcal{R} \partial_i \psi + \mathcal{R} \dot{\mathcal{R}} \partial^2 \psi \right) \right. \\ & - 6F_\chi \partial_i \mathcal{R} \partial_i \psi \frac{\partial^2\mathcal{R}}{a^2} + 2\mathcal{K} \partial_i \mathcal{R} \partial_i \psi \partial^2 \psi - F_\chi \frac{(\partial\mathcal{R})^2}{a^2} \partial^2 \psi + \frac{1}{2} \left(\tilde{f}_2 \mathcal{R} - \tilde{f}_3 \dot{\mathcal{R}} \right) (\partial^2 \psi)^2 \\ & - 2 \left(F_\chi \mathcal{R} - 3F_{\chi\chi} \dot{\mathcal{R}} \right) \frac{\partial^2\mathcal{R}}{a^2} \partial^2 \psi + \frac{3}{2} \left(F \mathcal{R} - F_\chi \dot{\mathcal{R}} \right) \partial_i \partial_j \psi \partial_i \partial_j \psi - F_{\chi\chi} \frac{\partial^2\mathcal{R}}{a^2} (\partial^2 \psi)^2 \\ & \left. - 3(2F_{\chi\chi} - 3HF_{\chi\chi\chi}) \dot{\mathcal{R}} \partial^2 \psi \partial^2 \psi \right\}, \quad (\text{A.10}) \end{aligned}$$

where, using the definition of \mathcal{K} in Eq. (2.9), the coefficients \tilde{f}_i are given by

$$\tilde{f}_1 \equiv F + 3HF_\chi + 9H^2 \epsilon_H F_{\chi\chi} \quad (\text{A.11})$$

$$\tilde{f}_2 \equiv 2\mathcal{K} - F - 9HF_\chi + 9H^2 F_{\chi\chi} (3 - 2\epsilon_H) + 27H^3 F_{\chi\chi\chi} \epsilon_H \quad (\text{A.12})$$

$$\tilde{f}_3 \equiv 2F_\chi - 9HF_{\chi\chi} \quad (\text{A.13})$$

The next step is to eliminate ψ in the above action by utilizing Eq. (A.5). To do this, let us define $\partial^2 \Xi \equiv Q_2 \dot{\mathcal{R}}$ in which $Q_2 \equiv 3\tilde{\nu}^2 / (1 + \tilde{\nu}^2)$ with $\tilde{\nu} = \sqrt{\mathcal{K}/F}$. This definition provides us with the contributions proportional to the linear differential equation of \mathcal{R} , i.e.,

$$\left. \frac{\delta \mathcal{L}_2}{\delta \mathcal{R}} \right|_1 = - \left[\partial_t \left(\vartheta a^3 \dot{\mathcal{R}} \right) - \vartheta a c_s^2 \partial^2 \mathcal{R} + \frac{\vartheta \sigma^2}{a} \partial^4 \mathcal{R} \right], \quad (\text{A.14})$$

in the final cubic action. Substituting the relation

$$\psi = \frac{Q_1}{H} \frac{\mathcal{R}}{a^2} + \Xi, \quad Q_1 \equiv -1 - c_s^2 Q_2 \quad (\text{A.15})$$

into the action (A.10) and performing a lot of integrations by parts and dropping the total derivative terms⁸, the corresponding cubic Lagrangian is obtained to be

$$\begin{aligned}
\frac{\mathcal{L}_3}{a^3} = & f_1 \mathcal{R} \frac{(\partial\mathcal{R})^2}{a^2} + f_2 \dot{\mathcal{R}} \frac{(\partial\mathcal{R})^2}{a^2} + f_3 \dot{\mathcal{R}}^2 \frac{\partial^2\mathcal{R}}{a^2} + f_4 \mathcal{R} \left(\frac{\partial^2\mathcal{R}}{a^2}\right)^2 + f_5 \dot{\mathcal{R}} \left(\frac{\partial^2\mathcal{R}}{a^2}\right)^2 \\
& + f_6 \left(\frac{\partial^2\mathcal{R}}{a^2}\right)^3 + f_7 \mathcal{R} \dot{\mathcal{R}}^2 + f_8 \dot{\mathcal{R}}^3 + f_9 \frac{\partial^2\mathcal{R}}{a^2} \frac{(\partial\mathcal{R})^2}{a^2} + f_{10} \dot{\mathcal{R}} \frac{\partial^2\dot{\mathcal{R}}}{a^2} \frac{\partial^2\mathcal{R}}{a^2} \\
& + f_{11} \dot{\mathcal{R}}^2 \frac{\partial^2\dot{\mathcal{R}}}{a^2} + f_{12} \left(\frac{\partial\mathcal{R}}{a}\right)^2 \frac{\partial^4\mathcal{R}}{a^4} + f_{13} \left(\frac{\partial\mathcal{R}}{a}\right)^2 \frac{\partial^2\dot{\mathcal{R}}}{a^2} + f_{14} \frac{\partial_i\mathcal{R}}{a} \partial^i\partial^j\Xi \frac{\partial_j\mathcal{R}}{a} \\
& + f_{15} \frac{\partial^2\mathcal{R}}{a^2} \partial_i\mathcal{R} \partial^i\Xi + f_{16} \dot{\mathcal{R}} \partial_i\mathcal{R} \partial^i\Xi + f_{17} \frac{\partial^4\mathcal{R}}{a^4} \partial_i\mathcal{R} \partial^i\Xi + f_{18} \partial^2\mathcal{R} (\partial\Xi)^2 \\
& + f_{19} \frac{\partial^2\dot{\mathcal{R}}}{a^2} \partial_i\mathcal{R} \partial^i\Xi + f_{20} \frac{\partial^2\mathcal{R}}{a^2} \partial_i\dot{\mathcal{R}} \partial^i\Xi + f_{21} \frac{\partial^2\mathcal{R}}{a^2} \partial_i\partial_j\Xi \frac{\partial^i\partial^j\mathcal{R}}{a^2} + f_{22} \frac{\partial^4\mathcal{R}}{a^2} (\partial\Xi)^2 \\
& + \mathcal{F} \left. \frac{\delta\mathcal{L}_2}{\delta\mathcal{R}} \right|_1.
\end{aligned} \tag{A.16}$$

in which the coefficient in front of $\delta\mathcal{L}_2/\delta\mathcal{R}|_1$ is

$$\mathcal{F} \equiv \frac{\epsilon_F}{\epsilon_H} \left[\frac{Q_2 - 3}{3H} (2Q_2\mathcal{R}\dot{\mathcal{R}} - \partial^{-2}\partial^i\partial^j(\partial_i\mathcal{R}\partial_j\Xi)) + 3\partial_i\mathcal{R}\partial^i\Xi - \frac{Q_1\kappa}{a^2H^2} \partial^{-2}\partial^i\partial^j(\partial_i\mathcal{R}\partial_j\mathcal{R}) \right].$$

Here ∂^{-2} is the inverse Laplacian and $\kappa \equiv \epsilon_F/\epsilon_H + \epsilon_F^{(2)}/\epsilon_H - \epsilon_H^{(2)}/\epsilon_H$. Clearly, all contributions in \mathcal{F} include time and spatial derivatives of \mathcal{R} which vanishes in the large-scale limit ($k \rightarrow 0$). When we calculate the bispectrum, we neglect the last term in cubic Lagrangian (A.16) relative to those coming from other terms. The other coefficients are given by

$$\begin{aligned}
f_1 = & \frac{\mathcal{K}}{\tilde{\nu}^2} \left\{ 1 + Q_1Q_2 \left(1 - \frac{\epsilon_F}{\epsilon_H}\right) (1 + \epsilon_{Q_1} + \epsilon_{Q_2}) + \frac{1}{3}\epsilon_F (1 + \kappa) (3 - 4Q_2 + Q_2^2(1 + Q_1)) \right. \\
& + \left. \frac{1}{3}\frac{\epsilon_F}{\epsilon_H} \mathcal{D}_1 + \epsilon_H Q_1Q_2 \left(1 - \frac{\epsilon_F}{\epsilon_H}\kappa\right) + \frac{Q_1Q_2}{2}\epsilon_F \left((4 + \epsilon_{Q_1} + \epsilon_{Q_2}) \mathcal{C}_1 + \mathcal{C}_2\epsilon_H \right) \right\} \\
& - 3\mathcal{K}Q_1(1 + \epsilon_H + \epsilon_{Q_1}) + \mathcal{K}Q_1Q_2(1 + \epsilon_H + \epsilon_{Q_1} + \epsilon_{Q_2}),
\end{aligned} \tag{A.17}$$

$$\begin{aligned}
f_2 = & \frac{\mathcal{K}}{H} \left(Q_1 + \frac{Q_2}{6\tilde{\nu}^2} \frac{\epsilon_F}{\epsilon_H} \right) (Q_2 - 3) + \frac{\mathcal{K}Q_1Q_2}{2H\tilde{\nu}^2} \left\{ 1 - \frac{\epsilon_F}{\epsilon_H} \left(2 + 3\frac{\epsilon_F}{\epsilon_H} + 3\frac{\epsilon_F^{(2)}}{\epsilon_H} - 3\frac{\epsilon_H^{(2)}}{\epsilon_H} + \frac{Q_2}{3} \right) \right. \\
& \left. + \mathcal{C}_3\epsilon_H \right\},
\end{aligned}$$

$$\begin{aligned}
f_3 = & \frac{\mathcal{K}}{36H^2\tilde{\nu}^2} \frac{\epsilon_F}{\epsilon_H} \left\{ Q_1Q_2 \left(3(Q_2 - 5) + 36\kappa + 6B(-5 - \epsilon_H + \epsilon_{Q_1} + \epsilon_{Q_2}) \right) + 6\mathcal{C}_4\epsilon_H \right. \\
& \left. - 4(1 + \kappa)(Q_2 - 3)^2 \right\},
\end{aligned}$$

⁸The integration by parts relations presented in Ref. [87] are useful in simplifying the calculations of the cubic action.

$$f_4 = \frac{\mathcal{K}Q_1^2}{H^2} \left(1 + \frac{1}{\tilde{\nu}^2}\right) + \frac{\mathcal{K}Q_1}{18H^2\tilde{\nu}^2} \left\{ 3(9Q_1\kappa - 4) \frac{\epsilon_F}{\epsilon_H} + 9Q_1\epsilon_F (4\kappa^2 + 2\kappa(1 - \frac{\epsilon_F^{(2)}}{\epsilon_H})) - \mathcal{C}_1 \right. \\ \left. - 2Q_2 \left(\frac{\epsilon_F}{\epsilon_H}\right)^2 [Q_2\epsilon_{Q_2} + (Q_2 - 3)(-1 + \epsilon_{Q_1} + \epsilon_{Q_2} + \epsilon_H(3 + 2\kappa - \frac{\epsilon_F}{\epsilon_H}))] \right\},$$

$$f_5 = \frac{\mathcal{K}Q_1}{18H^3\tilde{\nu}^2} \frac{\epsilon_F}{\epsilon_H} \left\{ (Q_2 - 3) \left(Q_2 \frac{\epsilon_F}{\epsilon_H} - 4(1 + \kappa)\right) + 6Q_1(4\kappa^2 + 2\kappa(1 - \frac{\epsilon_F^{(2)}}{\epsilon_H})) - \mathcal{C}_1 \right. \\ \left. - 3Q_1(2 - 3\kappa) \right\},$$

$$f_6 = -\frac{\mathcal{K}Q_1^2}{9H^4\tilde{\nu}^2} \frac{\epsilon_F}{\epsilon_H} \left(1 + \kappa + \frac{3}{2} \left(\frac{\epsilon_F}{\epsilon_H}\right) \kappa - \frac{Q_1}{4}\right),$$

$$f_7 = \frac{\mathcal{K}Q_2}{2\tilde{\nu}^2} \left\{ 18 \frac{\epsilon_F}{\epsilon_H} + 2Q_2 + Q_2 \left(\frac{\epsilon_F}{\epsilon_H}\right)^2 \left(\frac{\epsilon_F^{(2)}}{\epsilon_H} - \frac{\epsilon_F^{(3)}}{\epsilon_H}\right) \epsilon_H + \frac{1}{3} \frac{\epsilon_F}{\epsilon_H} Q_2^2 (6 - (\epsilon_H(1 + \kappa) + \epsilon_{Q_2})) \right\} \\ + \mathcal{K}(Q_2 - 3)^2 + \frac{2}{3} \left(\frac{\epsilon_F}{\epsilon_H}\right)^2 Q_2^2 (Q_2 - 3) \epsilon_H,$$

$$f_8 = -\frac{\mathcal{K}Q_2^2}{9H\tilde{\nu}^2} \frac{\epsilon_F}{\epsilon_H} \left\{ 3 - \frac{9}{2}\kappa - Q_2 + (3 - \epsilon_{Q_2})(4\kappa^2 + 2\kappa(1 - \frac{\epsilon_F^{(2)}}{\epsilon_H})) - \mathcal{C}_1 + \mathcal{C}_8 \epsilon_H \right\},$$

$$f_9 = -\frac{\mathcal{K}Q_1}{12H^2\tilde{\nu}^2} \left\{ -27Q_1 + 2 \left(\frac{\epsilon_F}{\epsilon_H}\right)^2 Q_2 (Q_2 - 3) (-1 + \epsilon_{Q_1} + \epsilon_{Q_2} + \epsilon_H(3 - \frac{\epsilon_F}{\epsilon_H} + 2\kappa)) \right. \\ \left. + \frac{\epsilon_F}{\epsilon_H} [28 + 15\kappa + Q_1\mathcal{D}_2] + 2Q_2^2 \left(\frac{\epsilon_F}{\epsilon_H}\right)^2 \epsilon_{Q_2} \right\} + \frac{2\mathcal{K}Q_1^2}{H^2},$$

$$f_{10} = \frac{\mathcal{K}Q_1^2}{3H^4\tilde{\nu}^2} \frac{\epsilon_F}{\epsilon_H} \mathcal{C}_9, \quad f_{11} = \frac{HQ_2}{2Q_1} f_{10}, \quad f_{12} = \frac{\mathcal{K}Q_1^3}{12H^4\tilde{\nu}^2} \frac{\epsilon_F}{\epsilon_H}, \quad f_{13} = -\frac{\mathcal{K}Q_1Q_2(Q_2 - 3)}{6H^3\tilde{\nu}^2} \left(\frac{\epsilon_F}{\epsilon_H}\right)^2$$

$$f_{14} = \frac{3\mathcal{K}Q_1}{H\tilde{\nu}^2} \frac{\epsilon_F}{\epsilon_H}, \quad f_{15} = \frac{Q_1}{H} (2\mathcal{K} + \kappa \left(\frac{\epsilon_F}{\epsilon_H}\right)^2 \epsilon_H),$$

$$f_{16} = (Q_2 - 3) (2\mathcal{K} + Q_2 \left(\frac{\epsilon_F}{\epsilon_H}\right)^2 \epsilon_H) + \frac{\mathcal{K}}{6\tilde{\nu}^2} [(54 + 5Q_2^2\epsilon_{Q_2}) \frac{\epsilon_F}{\epsilon_H} - 5Q_2(Q_2 - 3)(1 + \kappa)\epsilon_F],$$

$$f_{17} = -\frac{2}{Q_2} f_{13}, \quad f_{18} = \frac{1}{6} (Q_2 - 3) \left(\frac{\epsilon_F}{\epsilon_H}\right)^2 \epsilon_H + \frac{\mathcal{K}}{6\tilde{\nu}^2} (9 - \frac{\epsilon_F}{\epsilon_H} Q_2 \epsilon_{Q_2} - (Q_2 - 3)(1 + \kappa)\epsilon_F),$$

$$f_{19} = -\frac{\mathcal{K}Q_1}{H^2\tilde{\nu}^2} \left(\frac{1}{2} + \kappa - \frac{Q_2}{6}\right) \frac{\epsilon_F}{\epsilon_H}, \quad f_{20} = f_{19} - \frac{\mathcal{K}Q_1Q_2}{6H^2\tilde{\nu}^2} \frac{\epsilon_F}{\epsilon_H}$$

$$f_{21} = \frac{\mathcal{K}Q_1}{9H^3\bar{\nu}^2}(3Q_1 - (Q_2 - 3)\frac{\epsilon_F}{\epsilon_H})\frac{\epsilon_F}{\epsilon_H}, \quad f_{22} = \left(\frac{H}{Q_1}\right)^2 f_{12}$$

in which

$$\begin{aligned} \mathcal{C}_1 &= \kappa^2 + \kappa\left(1 + \frac{\epsilon_F}{\epsilon_H} + \frac{\epsilon_F^{(3)}}{\epsilon_H} - \frac{\epsilon_H^{(2)}}{\epsilon_H}\right) + \left(\frac{\epsilon_F}{\epsilon_H}\right)^2 + \frac{\epsilon_F}{\epsilon_H}\left(\frac{\epsilon_F^{(3)}}{\epsilon_H} - \frac{\epsilon_H^{(2)}}{\epsilon_H}\right) + \frac{\epsilon_H^{(2)}}{\epsilon_H}\left(\frac{\epsilon_H^{(3)}}{\epsilon_H} - \frac{\epsilon_F^{(3)}}{\epsilon_H}\right) \\ \mathcal{C}_2 &= \kappa^3 + \left(\frac{\epsilon_F}{\epsilon_H}\right)^3 + 2\left(2\frac{\epsilon_F}{\epsilon_H} + \frac{\epsilon_F^{(2)}}{\epsilon_H}\right)\kappa^2 + \left(3 - 5\frac{\epsilon_F}{\epsilon_H} - 2\frac{\epsilon_F^{(3)}}{\epsilon_H} + 4\frac{\epsilon_H^{(2)}}{\epsilon_H}\right)\frac{\epsilon_F}{\epsilon_H}\kappa + 2\left(1 - 2\frac{\epsilon_H^{(2)}}{\epsilon_H} - \frac{\epsilon_H^{(3)}}{\epsilon_H}\right)\kappa \\ &\quad + \left(3\frac{\epsilon_F^{(3)}}{\epsilon_H} + \left(\frac{\epsilon_F^{(3)}}{\epsilon_H}\right)^2 + \frac{\epsilon_F^{(3)}}{\epsilon_H}\frac{\epsilon_F^{(4)}}{\epsilon_H} - \frac{\epsilon_H^{(2)}}{\epsilon_H} + 2\frac{\epsilon_F^{(3)}}{\epsilon_H}\frac{\epsilon_H^{(2)}}{\epsilon_H}\right)\left(\kappa - \frac{\epsilon_F}{\epsilon_H}\right) + \left(3 + \frac{\epsilon_F}{\epsilon_H} - \frac{\epsilon_H^{(2)}}{\epsilon_H}\right)\left(\kappa^2 - \left(\frac{\epsilon_F}{\epsilon_H}\right)^2\right) \\ &\quad + \frac{\epsilon_H^{(2)}}{\epsilon_H}\left(\left(\frac{\epsilon_F^{(3)}}{\epsilon_H}\right)^2 - \left(\frac{\epsilon_H^{(3)}}{\epsilon_H}\right)^2\right) + \left(3 - \frac{\epsilon_H^{(2)}}{\epsilon_H}\right)\left(\frac{\epsilon_F^{(3)}}{\epsilon_H} - \frac{\epsilon_H^{(3)}}{\epsilon_H}\right) + \left(\frac{\epsilon_F^{(3)}}{\epsilon_H}\frac{\epsilon_F^{(4)}}{\epsilon_H} - \frac{\epsilon_H^{(3)}}{\epsilon_H}\frac{\epsilon_H^{(4)}}{\epsilon_H}\right) + 2\left(1 + 2\frac{\epsilon_F^{(3)}}{\epsilon_H}\right)\frac{\epsilon_F}{\epsilon_H} \\ \mathcal{C}_3 &= \left(\frac{\epsilon_F}{\epsilon_H} + \frac{\epsilon_F^{(2)}}{\epsilon_H}\right)^2 + \left(\frac{\epsilon_F}{\epsilon_H} + \frac{\epsilon_F^{(2)}}{\epsilon_H}\right)\left(1 - 3\frac{\epsilon_H^{(2)}}{\epsilon_H}\right) + \frac{\epsilon_F^{(2)}}{\epsilon_H}\left(\frac{\epsilon_F}{\epsilon_H} + \frac{\epsilon_F^{(3)}}{\epsilon_H}\right) + \frac{\epsilon_H^{(2)}}{\epsilon_H}\left(-1 + 2\frac{\epsilon_H^{(2)}}{\epsilon_H} - \frac{\epsilon_H^{(3)}}{\epsilon_H}\right) \\ \mathcal{C}_4 &= \left(\left(\frac{\epsilon_F}{\epsilon_H}\right)^2 + \left(\frac{\epsilon_F^{(2)}}{\epsilon_H}\right)^2\right)\left(1 - 6\frac{\epsilon_H^{(2)}}{\epsilon_H}\right) + \frac{\epsilon_F^{(2)}}{\epsilon_H}\left(3\left(\frac{\epsilon_F}{\epsilon_H}\right)^2 + \frac{\epsilon_F^{(3)}}{\epsilon_H}\left(3\frac{\epsilon_F^{(2)}}{\epsilon_H} + \frac{\epsilon_F^{(3)}}{\epsilon_H} + \frac{\epsilon_F^{(4)}}{\epsilon_H}\right)\right) \\ &\quad + \frac{\epsilon_F^{(2)}}{\epsilon_H}\left(3\frac{\epsilon_F}{\epsilon_H} + \frac{\epsilon_F^{(3)}}{\epsilon_H}\right)\left(1 - 6\frac{\epsilon_H^{(2)}}{\epsilon_H}\right) + \frac{\epsilon_H^{(2)}}{\epsilon_H}\left(\frac{\epsilon_F}{\epsilon_H} + \frac{\epsilon_F^{(2)}}{\epsilon_H}\right)\left(-3 + 11\frac{\epsilon_H^{(2)}}{\epsilon_H} - 4\frac{\epsilon_H^{(3)}}{\epsilon_H}\right) \\ &\quad + 2\left(1 - 3\frac{\epsilon_H^{(2)}}{\epsilon_H}\right)\left(\frac{\epsilon_H^{(2)}}{\epsilon_H}\right)^2 + \frac{\epsilon_H^{(2)}}{\epsilon_H}\frac{\epsilon_H^{(3)}}{\epsilon_H}\left(-1 + 7\frac{\epsilon_H^{(2)}}{\epsilon_H} + \frac{\epsilon_H^{(3)}}{\epsilon_H} - \frac{\epsilon_H^{(4)}}{\epsilon_H}\right) + \left(\frac{\epsilon_F}{\epsilon_H} + \frac{\epsilon_F^{(2)}}{\epsilon_H}\right)^3 \\ &\quad + 4\left(\frac{\epsilon_F^{(2)}}{\epsilon_H} + \frac{\epsilon_F^{(3)}}{\epsilon_H}\right)\frac{\epsilon_F}{\epsilon_H}\frac{\epsilon_F^{(2)}}{\epsilon_H} \\ \mathcal{C}_8 &= \left(\frac{\epsilon_F}{\epsilon_H}\right)^3 + 2\left(\frac{\epsilon_H^{(2)}}{\epsilon_H}\right)^3 + \left(3 + 4\frac{\epsilon_F}{\epsilon_H} + 3\frac{\epsilon_F^{(3)}}{\epsilon_H} - 3\frac{\epsilon_H^{(2)}}{\epsilon_H}\right)\kappa^2 - \left(3 + 5\kappa + \frac{\epsilon_F^{(3)}}{\epsilon_H} - \frac{\epsilon_H^{(2)}}{\epsilon_H}\right)\left(\frac{\epsilon_F}{\epsilon_H}\right)^2 \\ &\quad + \frac{\epsilon_F^{(3)}}{\epsilon_H}\left(2\frac{\epsilon_H^{(2)}}{\epsilon_H} - \frac{\epsilon_F^{(2)}}{\epsilon_H}\right)\left(3 + \frac{\epsilon_F}{\epsilon_H} + \frac{\epsilon_F^{(4)}}{\epsilon_H}\right) + \left(2 + 3\frac{\epsilon_F}{\epsilon_H} - \frac{\epsilon_F}{\epsilon_H}\frac{\epsilon_F^{(3)}}{\epsilon_H} + 2\frac{\epsilon_F}{\epsilon_H}\frac{\epsilon_H^{(2)}}{\epsilon_H} - 4\frac{\epsilon_H^{(2)}}{\epsilon_H}\frac{\epsilon_H^{(3)}}{\epsilon_H}\right)\kappa \\ &\quad - 6\left(\frac{\epsilon_H^{(2)}}{\epsilon_H}\right)^2 + \frac{\epsilon_H^{(2)}}{\epsilon_H}\left(3\frac{\epsilon_F^{(2)}}{\epsilon_H} - 2\frac{\epsilon_H^{(2)}}{\epsilon_H}\frac{\epsilon_F^{(2)}}{\epsilon_H} + 4\frac{\epsilon_F}{\epsilon_H}\frac{\epsilon_F^{(3)}}{\epsilon_H} - \frac{\epsilon_H^{(3)}}{\epsilon_H}\left(3 - 3\frac{\epsilon_H^{(2)}}{\epsilon_H} + \frac{\epsilon_H^{(3)}}{\epsilon_H} + \frac{\epsilon_H^{(4)}}{\epsilon_H}\right)\right) + \kappa^3 \\ \mathcal{C}_9 &= \kappa^2 + \left(1 - \frac{\epsilon_H^{(2)}}{\epsilon_H}\right)\kappa + \frac{\epsilon_F^{(2)}}{\epsilon_H}\left(\frac{\epsilon_F}{\epsilon_H} + \frac{\epsilon_F^{(3)}}{\epsilon_H}\right) - \frac{\epsilon_H^{(2)}}{\epsilon_H}\frac{\epsilon_H^{(3)}}{\epsilon_H} \\ \mathcal{D}_1 &= 3 - 4Q_2(1 + \epsilon_{Q_2}) + Q_2^2(1 + 2\epsilon_{Q_2}) + Q_1Q_2^2(1 + \epsilon_{Q_1} + 2\epsilon_{Q_2}) + \frac{3}{2}Q_1Q_2(1 + \epsilon_{Q_1} + \epsilon_{Q_2}) \\ \mathcal{D}_2 &= 3 - 6\epsilon_{Q_1} + 15\kappa - 3\epsilon_H(3 + \kappa) + Q_2(-1 + 2\epsilon_{Q_1} + \epsilon_{Q_2} + \epsilon_H(3 + \kappa)) \end{aligned}$$

B Explicit expressions for the amplitude of bispectrum

Using Eqs. (4.1) and (A.16) and the definition of $\mathcal{I}_{n_1, n_2}^{p_1, p_2, p_3}$ in Eq. (4.10), it is possible to write down explicitly form of the the non-Gaussian amplitude \mathcal{A} defined in Eq. (4.3) for each term

of the cubic Lagrangian (A.16) as follows:

$$\mathcal{A}^{(1)} = \frac{f_1 H^4}{c_s^8 \mathcal{P}_{\mathcal{R}}^2 \vartheta^3} k_1 \mathcal{I}_{1,-2}^{0,0,0} \sum_{i,j,l=1}^3 |\epsilon_{ijl}| \mathbf{k}_i \cdot \mathbf{k}_j \quad (\text{B.1})$$

$$\mathcal{A}^{(4)} = \frac{f_4 H^6}{c_s^{10} \mathcal{P}_{\mathcal{R}}^2 \vartheta^3} \frac{1}{k_1} \mathcal{I}_{2,0}^{0,0,0} \sum_{i,j,l=1}^3 |\epsilon_{ijl}| k_i^2 k_j^2 \quad (\text{B.2})$$

$$\mathcal{A}^{(6)} = \frac{6 f_6 H^8}{c_s^{12} \mathcal{P}_{\mathcal{R}}^2 \vartheta^3} \frac{k_2^2 k_3^2}{k_1 \sum_{i=1}^3 k_i^3} \mathcal{I}_{3,2}^{0,0,0} \quad (\text{B.3})$$

$$\mathcal{A}^{(9)} = \frac{f_9 H^8}{c_s^{10} \mathcal{P}_{\mathcal{R}}^2 \vartheta^3} \frac{1}{k_1} \mathcal{I}_{2,0}^{0,0,0} \sum_{i,j,l=1}^3 |\epsilon_{ijl}| k_i^2 (\mathbf{k}_j \cdot \mathbf{k}_l) \quad (\text{B.4})$$

$$\mathcal{A}^{(11)} = \frac{2 f_{11} H^7}{c_s^8 \mathcal{P}_{\mathcal{R}}^2 \vartheta^3} \frac{k_2 k_3 \sum_{i=1}^3 k_i^2}{k_1} \mathcal{I}_{1,1}^{1,1,1} \quad (\text{B.5})$$

$$\mathcal{A}^{(12)} = \frac{f_{12} H^8}{c_s^{12} \mathcal{P}_{\mathcal{R}}^2 \vartheta^3} \frac{1}{k_1^3} \mathcal{I}_{3,2}^{0,0,0} \sum_{i,j,l=1}^3 |\epsilon_{ijl}| k_i^4 (\mathbf{k}_j \cdot \mathbf{k}_l). \quad (\text{B.6})$$

For the case of $p_1 = 1$ and $p_2 = p_3 = 0$, we have

$$\mathcal{A}^{(5)} = \frac{f_5 H^7}{c_s^{10} \mathcal{P}_{\mathcal{R}}^2 \vartheta^3} k_2^2 k_3^2 \sum_{i,j,l=1}^3 |\epsilon_{ijl}| \mathcal{I}_{2,1}^{p_i, p_j, p_l} k_i^{-1} \quad (\text{B.7})$$

$$\mathcal{A}^{(13)} = \frac{f_{13} H^7}{c_s^{10} \mathcal{P}_{\mathcal{R}}^2 \vartheta^3} \frac{1}{k_1^2} \sum_{i,j,l=1}^3 |\epsilon_{ijl}| \mathcal{I}_{2,1}^{p_i, p_j, p_l} k_i^3 (\mathbf{k}_j \cdot \mathbf{k}_l) \quad (\text{B.8})$$

$$\mathcal{A}^{(14)} = \frac{Q_2 f_{14} H^5}{c_s^8 \mathcal{P}_{\mathcal{R}}^2 \vartheta^3} \sum_{i,j,l=1}^3 |\epsilon_{ijl}| \mathcal{I}_{1,-1}^{p_i, p_j, p_l} \frac{(\mathbf{k}_j \cdot \mathbf{k}_i)(\mathbf{k}_i \cdot \mathbf{k}_l)}{k_i} \quad (\text{B.9})$$

$$\mathcal{A}^{(15)} = \frac{Q_2 f_{15} H^5}{c_s^8 \mathcal{P}_{\mathcal{R}}^2 \vartheta^3} \sum_{i,j,l=1}^3 |\epsilon_{ijl}| \mathcal{I}_{1,-1}^{p_i, p_j, p_l} \frac{(\mathbf{k}_i \cdot \mathbf{k}_j) k_l^2}{k_i} \quad (\text{B.10})$$

$$\mathcal{A}^{(17)} = \frac{Q_2 f_{17} H^7}{c_s^{10} \mathcal{P}_{\mathcal{R}}^2 \vartheta^3} \frac{1}{k_1^3 k_2 k_3} \sum_{i,j,l=1}^3 |\epsilon_{ijl}| \mathcal{I}_{2,1}^{p_i, p_j, p_l} (\mathbf{k}_i \cdot \mathbf{k}_j) k_j k_l^5 \quad (\text{B.11})$$

$$\mathcal{A}^{(21)} = \frac{Q_2 f_{21} H^7}{c_s^{10} \mathcal{P}_{\mathcal{R}}^2 \vartheta^3} \frac{1}{k_1^3 k_2 k_3} \sum_{i,j,l=1}^3 |\epsilon_{ijl}| \mathcal{I}_{2,1}^{p_i, p_j, p_l} (\mathbf{k}_i \cdot \mathbf{k}_j)^2 k_j k_l^3. \quad (\text{B.12})$$

Finally, for $p_1 = p_2 = 1$ and $p_3 = 0$, the rest of expressions are given by

$$\mathcal{A}^{(3)} = \frac{f_3 H^6}{c_s^8 \mathcal{P}_{\mathcal{R}}^2 \vartheta^3} k_2 k_3 \sum_{i,j,l=1}^3 |\epsilon_{ijl}| \mathcal{I}_{1,0}^{p_i, p_j, p_l} k_l \quad (\text{B.13})$$

$$\mathcal{A}^{(7)} = \frac{f_7 H^4}{c_s^6 \mathcal{P}_{\mathcal{R}}^2 \vartheta^3} k_1 \sum_{i,j,l=1}^3 |\epsilon_{ijl}| \mathcal{I}_{0,-2}^{p_i, p_j, p_l} k_i k_j \quad (\text{B.14})$$

$$\mathcal{A}^{(10)} = \frac{f_{10} H^8}{c_s^{10} \mathcal{P}_{\mathcal{R}}^2 \vartheta^3} \frac{k_2 k_3}{k_1^2} \sum_{i,j,l=1}^3 |\epsilon_{ijl}| \mathcal{I}_{2,2}^{p_i, p_j, p_l} (k_i^2 + k_j^2) k_l \quad (\text{B.15})$$

$$\mathcal{A}^{(16)} = \frac{Q_2 f_{16} H^4}{c_s^6 \mathcal{P}_{\mathcal{R}}^2 \vartheta^3} \frac{1}{k_2 k_3} \sum_{i,j,l=1}^3 |\epsilon_{ijl}| \mathcal{I}_{0,-2}^{p_i, p_j, p_l} k_i^2 (\mathbf{k}_j \cdot \mathbf{k}_l) k_l \quad (\text{B.16})$$

$$\mathcal{A}^{(18)} = \frac{Q_2^2 f_{18} H^4}{c_s^6 \mathcal{P}_{\mathcal{R}}^2 \vartheta^3} \frac{1}{k_2 k_3} \sum_{i,j,l=1}^3 |\epsilon_{ijl}| \mathcal{I}_{0,-2}^{p_i, p_j, p_l} (\mathbf{k}_i \cdot \mathbf{k}_j) k_l^3 \quad (\text{B.17})$$

$$\mathcal{A}^{(19)} = \frac{Q_2 f_{19} H^6}{c_s^8 \mathcal{P}_{\mathcal{R}}^2 \vartheta^3} \frac{1}{k_1^2 k_2 k_3} \sum_{i,j,l=1}^3 |\epsilon_{ijl}| \mathcal{I}_{1,0}^{p_i, p_j, p_l} (\mathbf{k}_i \cdot \mathbf{k}_l) k_j^4 k_l \quad (\text{B.18})$$

$$\mathcal{A}^{(20)} = \frac{Q_2 f_{20} H^6}{c_s^8 \mathcal{P}_{\mathcal{R}}^2 \vartheta^3} \frac{1}{k_1^2 k_2 k_3} \sum_{i,j,l=1}^3 |\epsilon_{ijl}| \mathcal{I}_{1,0}^{p_i, p_j, p_l} (\mathbf{k}_i \cdot \mathbf{k}_j) (k_i^2 + k_j^2) k_l^3 \quad (\text{B.19})$$

$$\mathcal{A}^{(22)} = \frac{Q_2^2 f_{22} H^6}{c_s^8 \mathcal{P}_{\mathcal{R}}^2 \vartheta^3} \frac{1}{k_1^2 k_2 k_3} \sum_{i,j,l=1}^3 |\epsilon_{ijl}| \mathcal{I}_{1,0}^{p_i, p_j, p_l} (\mathbf{k}_i \cdot \mathbf{k}_j) k_l^5. \quad (\text{B.20})$$

B.1 Expansion in terms of slow-roll parameters

In order to derive a simple expression for f_{NL} in the equilateral configuration to the order of the slow roll parameter ϵ_H , let us first consider all terms defined in Eq. (2.19) to be much smaller than unity and $\tilde{\nu} \lesssim \mathcal{O}(\sqrt{\epsilon_H})$. Then the amplitude of non-Gaussianities can be written as

$$\mathcal{A}^{(j)} = B_j S^{(j)}, \quad (\text{B.21})$$

where B_j are the coefficients coming in front of each shape function $S^{(j)}$ for the amplitude $\mathcal{A}^{(j)}$ listed in previous subsection, for example $B_1 = f_1 H^4 / (c_s^8 \mathcal{P}_{\mathcal{R}}^2 \vartheta^3)$. With this decomposition, the shape coefficients can be expanded as shown in Table. 2. Correspondingly, the leading

Coefficient	B_1	B_2	B_3	B_4
Expansion	$-B_2(2c_s^2 + 3)$	$\frac{\eta}{\varrho^2}$	$\frac{B_2}{2}(4c_s^2 - 7)$	$\frac{11}{9}\frac{\eta}{\varrho^4}$
Coefficient	$B_5 \approx \frac{30c_s^2 B_6}{7}$	B_7	B_8	B_9
Expansion	$\frac{5}{11}B_4$	$-12c_s^2 B_2$	5η	$\frac{6}{7}c_s^2 B_6$
Coefficient	B_{10}	B_{11}	B_{12}	B_{13}
Expansion	$-\frac{2}{9}\left(3 + \frac{1}{c_s^2}\right)B_2$	$\frac{1}{15}\left(3 + \frac{1}{c_s^2}\right)B_8$	$\frac{1}{22c_s^2}B_4$	$-\frac{1}{c_s^2}B_2$
Coefficient	B_{14}	B_{15}	B_{16}	B_{17}
Expansion	$\frac{18}{11}c_s^2 \epsilon_H B_4$	$\left(\frac{2}{3\mathcal{K}}B_2 + \frac{6}{11}c_s^2 B_4\right)\epsilon_H^2$	$-\frac{54}{11}c_s^4 B_4 \epsilon_H$	$\frac{6}{11}B_4 \epsilon_H$
Coefficient	B_{18}	$B_{19} \approx B_{20}$	B_{21}	B_{22}
Expansion	$\frac{9}{11}c_s^4 B_4 \epsilon_H^2 + \frac{1}{3\mathcal{K}}c_s^2 B_2 \epsilon_H^3$	$\frac{3}{11}c_s^2 B_4 \epsilon_H$	$-\frac{4}{11}B_4 \epsilon_H$	$\frac{1}{22}c_s^2 B_4 \epsilon_H^2$

Table 2. The expansion of the shape function coefficient $B_{(i)}$ in terms of the slow-roll parameter ϵ_H . Here we have defined $\eta \equiv \frac{\pi^2 r_i^2}{72 c_s^6 \tilde{\nu}^2}$ and $\varrho \equiv c_s \tilde{\nu}$.

contribution to $f_{\text{NL}}^{\text{equi}}$ is obtained to be

$$\begin{aligned}
\frac{c_s^6 \tilde{\nu}^4}{\pi^4 r_t^2} f_{\text{NL}}^{\text{equi,lead}} &\simeq -\frac{1}{36} \left(2 + \frac{3}{c_s^2}\right) \mathcal{I}_{1,-2}^{0,0,0} - \frac{1}{81c_s^2} \left(3 + \frac{1}{c_s^2}\right) \mathcal{I}_{2,2}^{1,1,0} \\
&+ \frac{5}{972c_s^6 \tilde{\nu}^2} \mathcal{I}_{3,2}^{0,0,0} + \frac{1}{27c_s^4 \tilde{\nu}^2} \mathcal{I}_{2,0}^{0,0,0} + \frac{5\tilde{\nu}^2}{36} \mathcal{I}_{0,-1}^{1,1,1} + \frac{\tilde{\nu}^2}{108} \left(3 + \frac{1}{c_s^2}\right) \mathcal{I}_{1,1}^{1,1,1} \\
&+ \frac{1}{324c_s^4 \tilde{\nu}^2} (5 - 9\tilde{\nu}^2) \mathcal{I}_{2,1}^{1,0,0} + \frac{1}{36c_s^2} \mathcal{I}_{1,-1}^{1,0,0} - \frac{1}{3} \mathcal{I}_{0,-2}^{1,1,0} + \frac{1}{72} \left(4 - \frac{7}{c_s^2}\right) \mathcal{I}_{1,0}^{1,1,0} \\
&+ \frac{\epsilon_H}{\tilde{\nu}^2} \left[\frac{1}{162c_s^4} \mathcal{I}_{2,1}^{1,0,0} + \frac{1}{18c_s^2} \mathcal{I}_{1,-1}^{1,0,0} + \frac{1}{36c_s^2} \mathcal{I}_{1,0}^{1,1,0} - \frac{1}{6} \mathcal{I}_{0,-2}^{1,1,0} \right] + \frac{\epsilon_H^2}{\mathcal{K}c_s^2} \mathcal{I}_{1,-1}^{1,0,0} - \frac{\epsilon_H^3}{\mathcal{K}} \mathcal{I}_{0,-2}^{1,1,0}.
\end{aligned} \tag{B.22}$$

It worth mentioning that one can not discard the sub-leading orders of the slow-roll parameter relative to the leading order, because integral functions $\mathcal{I}_{n,m}^{p,q,r}$ and $\tilde{\nu}$ are running with ν .

It is interesting that the relative error in this approximation is

$$\delta = \left| \frac{f_{\text{NL}}^{\text{equi,lead}} - f_{\text{NL}}^{\text{equi}}}{f_{\text{NL}}^{\text{equi}}} \right| \ll \mathcal{O}(\epsilon_H). \tag{B.23}$$

This means that the expansion coefficients presented in Table. 2 are near to their exact values with high accuracies. Having these shape coefficients in hand, one can calculate f_{NL} in other configurations by using the amplitudes presented in Appendix. B.

References

- [1] A. H. Chamseddine and V. Mukhanov, *Mimetic Dark Matter*, *JHEP* **11** (2013) 135, [1308.5410].
- [2] N. Deruelle and J. Rua, *Disformal Transformations, Veiled General Relativity and Mimetic Gravity*, *JCAP* **09** (2014) 002, [1407.0825].
- [3] F.-F. Yuan and P. Huang, *Induced geometry from disformal transformation*, *Phys. Lett. B* **744** (2015) 120–124, [1501.06135].
- [4] A. H. Chamseddine, V. Mukhanov and A. Vikman, *Cosmology with Mimetic Matter*, *JCAP* **1406** (2014) 017, [1403.3961].
- [5] A. H. Chamseddine and V. Mukhanov, *Resolving Cosmological Singularities*, *JCAP* **03** (2017) 009, [1612.05860].
- [6] A. H. Chamseddine and V. Mukhanov, *Nonsingular Black Hole*, *Eur. Phys. J. C* **77** (2017) 183, [1612.05861].
- [7] L. Mirzaghali and A. Vikman, *Imperfect Dark Matter*, *JCAP* **06** (2015) 028, [1412.7136].
- [8] R. Myrzakulov, L. Sebastiani, S. Vagnozzi and S. Zerbini, *Static spherically symmetric solutions in mimetic gravity: rotation curves and wormholes*, *Class. Quant. Grav.* **33** (2016) 125005, [1510.02284].
- [9] F. Arroja, N. Bartolo, P. Karmakar and S. Matarrese, *Cosmological perturbations in mimetic Horndeski gravity*, *JCAP* **04** (2016) 042, [1512.09374].
- [10] L. Sebastiani, S. Vagnozzi and R. Myrzakulov, *Mimetic gravity: a review of recent developments and applications to cosmology and astrophysics*, *Adv. High Energy Phys.* **2017** (2017) 3156915, [1612.08661].
- [11] J. Dutta, W. Khyllep, E. N. Saridakis, N. Tamanini and S. Vagnozzi, *Cosmological dynamics of mimetic gravity*, *JCAP* **02** (2018) 041, [1711.07290].
- [12] H. Saadi, *A Cosmological Solution to Mimetic Dark Matter*, *Eur. Phys. J. C* **76** (2016) 14, [1411.4531].
- [13] H. Firouzjahi, M. A. Gorji, S. A. Hosseini Mansoori, A. Karami and T. Rostami, *Two-field disformal transformation and mimetic cosmology*, *JCAP* **11** (2018) 046, [1806.11472].
- [14] M. A. Gorji, A. Allahyari, M. Khodadi and H. Firouzjahi, *Mimetic black holes*, *Phys. Rev. D* **101** (2020) 124060, [1912.04636].
- [15] J. Matsumoto, S. D. Odintsov and S. V. Sushkov, *Cosmological perturbations in a mimetic matter model*, *Phys. Rev. D* **91** (2015) 064062, [1501.02149].
- [16] D. Momeni, K. Myrzakulov, R. Myrzakulov and M. Raza, *Cylindrical solutions in Mimetic gravity*, *Eur. Phys. J. C* **76** (2016) 301, [1505.08034].
- [17] A. V. Astashenok and S. D. Odintsov, *From neutron stars to quark stars in mimetic gravity*, *Phys. Rev. D* **94** (2016) 063008, [1512.07279].
- [18] N. Sadeghnezhad and K. Nozari, *Braneworld Mimetic Cosmology*, *Phys. Lett. B* **769** (2017) 134–140, [1703.06269].

- [19] K. Nozari and N. Rashidi, *Mimetic DBI Inflation in Confrontation with Planck2018 data*, *Astrophys. J.* **882** (2019) 78, [1912.06050].
- [20] A. R. Solomon, V. Vardanyan and Y. Akrami, *Massive mimetic cosmology*, *Phys. Lett. B* **794** (2019) 135–142, [1902.08533].
- [21] L. Shen, Y. Zheng and M. Li, *Two-field mimetic gravity revisited and Hamiltonian analysis*, *JCAP* **12** (2019) 026, [1909.01248].
- [22] A. Ganz, N. Bartolo and S. Matarrese, *Towards a viable effective field theory of mimetic gravity*, *JCAP* **12** (2019) 037, [1907.10301].
- [23] M. de Cesare, *Reconstruction of Mimetic Gravity in a Non-Singular Bouncing Universe from Quantum Gravity*, *Universe* **5** (2019) 107, [1904.02622].
- [24] K. Nozari and N. Sadeghnezhad, *Braneworld mimetic $f(R)$ gravity*, *Int. J. Geom. Meth. Mod. Phys.* **16** (2019) 1950042.
- [25] M. de Cesare, *Limiting curvature mimetic gravity for group field theory condensates*, *Phys. Rev. D* **99** (2019) 063505, [1812.06171].
- [26] A. Ganz, P. Karmakar, S. Matarrese and D. Sorokin, *Hamiltonian analysis of mimetic scalar gravity revisited*, *Phys. Rev. D* **99** (2019) 064009, [1812.02667].
- [27] A. Ganz, N. Bartolo, P. Karmakar and S. Matarrese, *Gravity in mimetic scalar-tensor theories after GW170817*, *JCAP* **01** (2019) 056, [1809.03496].
- [28] A. Sheykhi and S. Grunau, *Topological black holes in mimetic gravity*, 1911.13072.
- [29] A. Sheykhi, *Mimetic gravity in $(2 + 1)$ -dimensions*, 2009.12826.
- [30] A. Sheykhi, *Mimetic Black Strings*, *JHEP* **07** (2020) 031, [2002.11718].
- [31] S. Nojiri and S. D. Odintsov, *Mimetic $F(R)$ gravity: inflation, dark energy and bounce*, 1408.3561.
- [32] A. V. Astashenok, S. D. Odintsov and V. Oikonomou, *Modified Gauss–Bonnet gravity with the Lagrange multiplier constraint as mimetic theory*, *Class. Quant. Grav.* **32** (2015) 185007, [1504.04861].
- [33] S. Nojiri, S. Odintsov and V. Oikonomou, *Unimodular-Mimetic Cosmology*, *Class. Quant. Grav.* **33** (2016) 125017, [1601.07057].
- [34] S. Nojiri, S. Odintsov and V. Oikonomou, *Ghost-Free $F(R)$ Gravity with Lagrange Multiplier Constraint*, *Phys. Lett. B* **775** (2017) 44–49, [1710.07838].
- [35] S. Nojiri, S. Odintsov and V. Oikonomou, *Viable Mimetic Completion of Unified Inflation–Dark Energy Evolution in Modified Gravity*, *Phys. Rev. D* **94** (2016) 104050, [1608.07806].
- [36] S. Odintsov and V. Oikonomou, *The reconstruction of $f(\phi)R$ and mimetic gravity from viable slow-roll inflation*, *Nucl. Phys. B* **929** (2018) 79–112, [1801.10529].
- [37] A. Casalino, M. Rinaldi, L. Sebastiani and S. Vagnozzi, *Alive and well: mimetic gravity and a higher-order extension in light of GW170817*, *Class. Quant. Grav.* **36** (2019) 017001, [1811.06830].
- [38] A. Barvinsky, *Dark matter as a ghost free conformal extension of Einstein theory*, *JCAP* **01** (2014) 014, [1311.3111].

- [39] M. Chaichian, J. Kluson, M. Oksanen and A. Tureanu, *Mimetic dark matter, ghost instability and a mimetic tensor-vector-scalar gravity*, *JHEP* **12** (2014) 102, [1404.4008].
- [40] A. Ijjas, J. Ripley and P. J. Steinhardt, *NEC violation in mimetic cosmology revisited*, *Phys. Lett. B* **760** (2016) 132–138, [1604.08586].
- [41] H. Firouzjahi, M. A. Gorji and S. A. Hosseini Mansoori, *Instabilities in Mimetic Matter Perturbations*, *JCAP* **1707** (2017) 031, [1703.02923].
- [42] S. Ramazanov, F. Arroja, M. Celoria, S. Matarrese and L. Pilo, *Living with ghosts in Hořava-Lifshitz gravity*, *JHEP* **06** (2016) 020, [1601.05405].
- [43] F. Capela and S. Ramazanov, *Modified Dust and the Small Scale Crisis in CDM*, *JCAP* **04** (2015) 051, [1412.2051].
- [44] A. De Felice and S. Mukohyama, *Phenomenology in minimal theory of massive gravity*, *JCAP* **04** (2016) 028, [1512.04008].
- [45] A. E. Gümrükçüoğlu, S. Mukohyama and T. P. Sotiriou, *Low energy ghosts and the Jeans’ instability*, *Phys. Rev. D* **94** (2016) 064001, [1606.00618].
- [46] E. Babichev and S. Ramazanov, *Gravitational focusing of Imperfect Dark Matter*, *Phys. Rev. D* **95** (2017) 024025, [1609.08580].
- [47] E. Babichev and S. Ramazanov, *Caustic free completion of pressureless perfect fluid and k-essence*, *JHEP* **08** (2017) 040, [1704.03367].
- [48] M. A. Gorji, S. Mukohyama, H. Firouzjahi and S. A. Hosseini Mansoori, *Gauge Field Mimetic Cosmology*, *JCAP* **08** (2018) 047, [1807.06335].
- [49] M. A. Gorji, S. Mukohyama and H. Firouzjahi, *Cosmology in Mimetic SU(2) Gauge Theory*, *JCAP* **05** (2019) 019, [1903.04845].
- [50] Y. Zheng, L. Shen, Y. Mou and M. Li, *On (in)stabilities of perturbations in mimetic models with higher derivatives*, *JCAP* **08** (2017) 040, [1704.06834].
- [51] S. Hirano, S. Nishi and T. Kobayashi, *Healthy imperfect dark matter from effective theory of mimetic cosmological perturbations*, *JCAP* **07** (2017) 009, [1704.06031].
- [52] M. A. Gorji, S. A. Hosseini Mansoori and H. Firouzjahi, *Higher Derivative Mimetic Gravity*, *JCAP* **01** (2018) 020, [1709.09988].
- [53] N. Arkani-Hamed, P. Creminelli, S. Mukohyama and M. Zaldarriaga, *Ghost inflation*, *JCAP* **0404** (2004) 001, [hep-th/0312100].
- [54] C. Cheung, P. Creminelli, A. Fitzpatrick, J. Kaplan and L. Senatore, *The Effective Field Theory of Inflation*, *JHEP* **03** (2008) 014, [0709.0293].
- [55] M. Alishahiha, E. Silverstein and D. Tong, *DBI in the sky*, *Phys. Rev. D* **70** (2004) 123505, [hep-th/0404084].
- [56] PLANCK collaboration, Y. Akrami et al., *Planck 2018 results. X. Constraints on inflation*, 1807.06211.
- [57] PLANCK collaboration, Y. Akrami et al., *Planck 2018 results. IX. Constraints on primordial non-Gaussianity*, 1905.05697.
- [58] Y. Zheng, *Hamiltonian analysis of Mimetic gravity with higher derivatives*, 1810.03826.

- [59] A. Golovnev, *On the recently proposed Mimetic Dark Matter*, *Phys. Lett.* **B728** (2014) 39–40, [1310.2790].
- [60] J. Khoury, B. A. Ovrut, P. J. Steinhardt and N. Turok, *The Ekpyrotic universe: Colliding branes and the origin of the hot big bang*, *Phys. Rev. D* **64** (2001) 123522, [hep-th/0103239].
- [61] R. Kallosh, L. Kofman and A. D. Linde, *Pyrotechnic universe*, *Phys. Rev. D* **64** (2001) 123523, [hep-th/0104073].
- [62] F. Finelli and R. Brandenberger, *On the generation of a scale invariant spectrum of adiabatic fluctuations in cosmological models with a contracting phase*, *Phys. Rev. D* **65** (2002) 103522, [hep-th/0112249].
- [63] E. I. Buchbinder, J. Khoury and B. A. Ovrut, *New Ekpyrotic cosmology*, *Phys. Rev. D* **76** (2007) 123503, [hep-th/0702154].
- [64] E. I. Buchbinder, J. Khoury and B. A. Ovrut, *On the initial conditions in new ekpyrotic cosmology*, *JHEP* **11** (2007) 076, [0706.3903].
- [65] A. D. Linde, *Fast roll inflation*, *JHEP* **11** (2001) 052, [hep-th/0110195].
- [66] J. B. Hartle, S. Hawking and T. Hertog, *Accelerated Expansion from Negative Λ* , 1205.3807.
- [67] T. Fujita, X. Gao and J. Yokoyama, *Spatially covariant theories of gravity: disformal transformation, cosmological perturbations and the Einstein frame*, *JCAP* **02** (2016) 014, [1511.04324].
- [68] S. Corley and T. Jacobson, *Hawking spectrum and high frequency dispersion*, *Phys. Rev.* **D54** (1996) 1568–1586, [hep-th/9601073].
- [69] S. Corley, *Computing the spectrum of black hole radiation in the presence of high frequency dispersion: An Analytical approach*, *Phys. Rev.* **D57** (1998) 6280–6291, [hep-th/9710075].
- [70] J. Martin and R. H. Brandenberger, *The TransPlanckian problem of inflationary cosmology*, *Phys. Rev.* **D63** (2001) 123501, [hep-th/0005209].
- [71] J. Martin and R. H. Brandenberger, *The Corley-Jacobson dispersion relation and transPlanckian inflation*, *Phys. Rev.* **D65** (2002) 103514, [hep-th/0201189].
- [72] A. Ashoorioon, D. Chialva and U. Danielsson, *Effects of Nonlinear Dispersion Relations on Non-Gaussianities*, *JCAP* **06** (2011) 034, [1104.2338].
- [73] A. Ashoorioon, R. Casadio, M. Cicoli, G. Geshnizjani and H. J. Kim, *Extended Effective Field Theory of Inflation*, *JHEP* **02** (2018) 172, [1802.03040].
- [74] A. Ashoorioon, *Non-Unitary Evolution in the General Extended EFT of Inflation | \mathcal{E} Excited Initial States*, *JHEP* **12** (2018) 012, [1807.06511].
- [75] M. Abramowitz and I. A. Stegun, *Handbook of mathematical functions with formulas, graphs, and mathematical tables*, vol. 55. US Government printing office, 1948.
- [76] X. Chen, M.-x. Huang, S. Kachru and G. Shiu, *Observational signatures and non-Gaussianities of general single field inflation*, *JCAP* **0701** (2007) 002, [hep-th/0605045].
- [77] LIGO SCIENTIFIC, VIRGO, FERMI-GBM, INTEGRAL collaboration, B. Abbott et al., *Gravitational Waves and Gamma-rays from a Binary Neutron Star Merger: GW170817 and GRB 170817A*, *Astrophys. J. Lett.* **848** (2017) L13, [1710.05834].

- [78] J. Sakstein and B. Jain, *Implications of the neutron star merger gw170817 for cosmological scalar-tensor theories*, *Phys. Rev. Lett.* **119** (Dec, 2017) 251303.
- [79] T. Baker, E. Bellini, P. G. Ferreira, M. Lagos, J. Noller and I. Sawicki, *Strong constraints on cosmological gravity from gw170817 and grb 170817a*, *Phys. Rev. Lett.* **119** (Dec, 2017) 251301.
- [80] J. Khoury, *Fading gravity and self-inflation*, *Phys. Rev. D* **76** (2007) 123513, [hep-th/0612052].
- [81] A. S. Koshelev, K. Sravan Kumar, A. Mazumdar and A. A. Starobinsky, *Non-Gaussianities and tensor-to-scalar ratio in non-local R^2 -like inflation*, *JHEP* **06** (2020) 152, [2003.00629].
- [82] E. Babichev, V. Mukhanov and A. Vikman, *k-Essence, superluminal propagation, causality and emergent geometry*, *JHEP* **02** (2008) 101, [0708.0561].
- [83] Y. Aharonov, A. Komar and L. Susskind, *Superluminal behavior, causality, and instability*, *Phys. Rev.* **182** (Jun, 1969) 1400–1403.
- [84] J. Garriga and V. F. Mukhanov, *Perturbations in k-inflation*, *Physics Letters B* **458** (1999) 219 – 225.
- [85] J. M. Maldacena, *Non-Gaussian features of primordial fluctuations in single field inflationary models*, *JHEP* **05** (2003) 013, [astro-ph/0210603].
- [86] V. Acquaviva, N. Bartolo, S. Matarrese and A. Riotto, *Second order cosmological perturbations from inflation*, *Nucl. Phys. B* **667** (2003) 119–148, [astro-ph/0209156].
- [87] A. De Felice and S. Tsujikawa, *Primordial non-Gaussianities in general modified gravitational models of inflation*, *JCAP* **04** (2011) 029, [1103.1172].